LMU-ASC 68/07

Hard spectator interactions in $B \to \pi\pi$ at order α_s^2

Volker Pilipp[1]
Arnold Sommerfeld Center, Department für Physik
Ludwig-Maximilians-Universität München
Theresienstrasse 37, 80333 München, Germany

Institute of Theoretical Physics
Universität Bern
Sidlerstrasse 5, 3012 Bern, Switzerland

Abstract

I compute the *hard spectator interaction* amplitude in $B \to \pi\pi$ at NLO i.e. at $\mathcal{O}(\alpha_s^2)$. This special part of the amplitude, whose LO starts at $\mathcal{O}(\alpha_s)$, is defined in the framework of QCD factorization. QCD factorization allows to separate the short- and the long-distance physics in leading power in an expansion in $\Lambda_{\rm QCD}/m_b$, where the short-distance physics can be calculated in a perturbative expansion in α_s.

In this calculation it is necessary to obtain an expansion of Feynman integrals in powers of $\Lambda_{\rm QCD}/m_b$. I will present a general method to obtain this expansion in a systematic way once the leading power is given as an input. This method is based on differential equation techniques and easy to implement in a computer algebra system.

The numerical impact on amplitudes and branching ratios is considered. The NLO contributions of the hard spectator interactions are important but small enough for perturbation theory to be valid.

1 Introduction

In the last decades B physics has proven to be a promising field to determine parameters of the flavour sector with high precision. On the theoretical side QCD factorization [1, 2] has turned out to be an appropriate tool to calculate B decay modes from first principles. Though the decay of the B-meson is caused by weak interactions, strong interactions play a dominant role. It is however not possible to handle the QCD effects completely perturbatively. This is due to the energy scales that are contained in the B-meson: Whereas α_s at the mass of the b-quark is a small parameter, the bound state of the quarks leads to an energy scale of $\mathcal{O}(\Lambda_{\rm QCD})$ which spoils perturbation theory. The idea of QCD factorization is to separate these scales. At leading power in $\Lambda_{\rm QCD}/m_b$ we obtain the amplitude for

[1] volker.pilipp@itp.unibe.ch

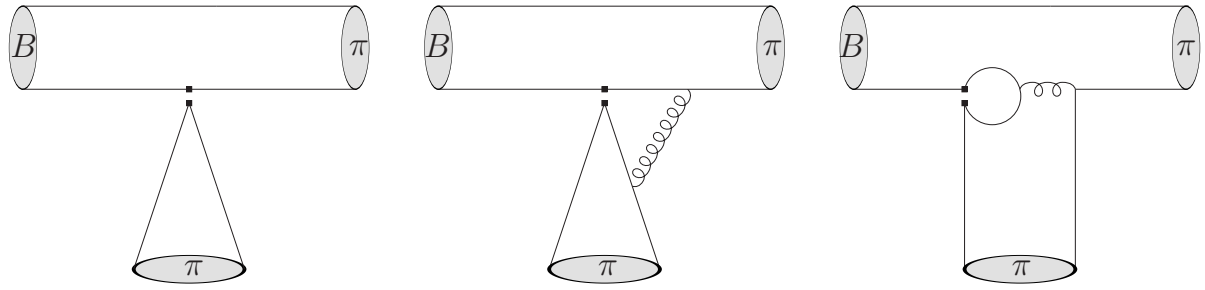

Figure 1: Tree level, vertex correction and penguin contraction. These diagrams contribute to T^{I}.

$B \to \pi\pi$ in the following form:

$$\begin{aligned}\langle\pi\pi|\mathcal{H}|B\rangle \;\sim\; & F^{B\to\pi}\int_0^1 dx\, T^{\mathrm{I}}(x) f_\pi\phi_\pi(x) + \\ & \int_0^1 dxdyd\xi\, T^{\mathrm{II}}(x,y,\xi) f_B\phi_{B1}(\xi) f_\pi\phi_\pi(x) f_\pi\phi_\pi(y) \qquad (1)\end{aligned}$$

Two different types of quantities enter this formula. On the one hand the hadronic physics is contained in the form factor $F^{B\to\pi}$ and the wave functions ϕ_{B1} and ϕ_π, which will be defined more precisely in the next section. These quantities contain the information about the bound states of the mesons. They have to be determined by non-perturbative methods like QCD sum rules or lattice calculations. Alternatively, because they are at least partly process independent, they might be extracted in the future from experiment. On the other hand the hard scattering kernels T^{I} and T^{II} contain the physics of the hard scale $\mathcal{O}(m_b)$ and the hard collinear scale $\mathcal{O}(\sqrt{m_b\Lambda_{\mathrm{QCD}}})$ and can be calculated perturbatively.

The Feynman diagrams that contribute to $B \to \pi\pi$ can be distributed into two different classes. The class of diagrams where there is no gluon line connecting the spectator quark with the rest of the diagram (fig. 1) contributes to T^{I}. We obtain T^{II} by evaluating the hard spectator scattering diagrams, which are shown in LO in α_s in fig. 2. The order α_s^2 corrections of T^{II} are the topic of the present work. Through the soft momentum l of the constituent quark of the B-meson the hard collinear scale $\sqrt{\Lambda_{\mathrm{QCD}} m_b}$ comes into play. This leads to the fact that in contrast to T^{I}, which is completely governed by the scale m_b, T^{II} comes with formally large logarithms. These logarithms cannot be resummed in the present QCD calculation. It will be shown by numerical analysis that the scale dependence of the hard spectator scattering amplitude and the absolute size of its NLO corrections are small enough for pertubation theory to be valid.

My calculation of the hard spectator scattering amplitude is not the first one as it has been calculated recently by [3, 4]. It is however the first pure QCD calculation, whereas [3, 4] used the framework of soft-collinear effective theory (SCET) [5, 6, 7] an effective theory, where the expansion in $\Lambda_{\mathrm{QCD}}/m_b$ is performed at the level of the Lagrangian rather than of Feynman integrals. It is the main result of this paper to confirm the results of [3, 4]

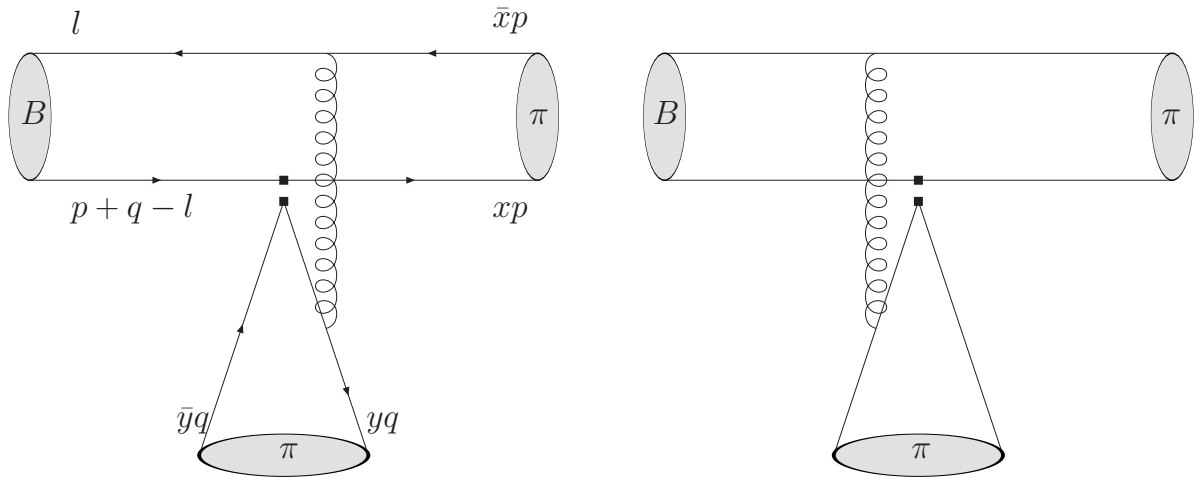

Figure 2: Hard spectator interactions at $\mathcal{O}(\alpha_s)$. This is the LO of T^{II}

and to show by explicit calculation that pure QCD and SCET lead to the same result in this case.

Hard spectator scattering corrections to the penguin diagram (third diagram of fig. 1) are beyond the scope of this publication. This class of diagrams does not influence the cancellation of the scale dependence of the "tree amplitude" i.e. the diagrams of fig. 2 and higher order α_s corrections. For phenomenological applications, however, the hard spectator penguin amplitudes, which have been recently calculated in [8], should be taken into account. Also the order α_s^2 of T^{I} is important for phenomenological applications. This calculation has been partly performed by [9, 10]. There the complete imaginary part and a preliminary result of the real part of the amplitude is given.

From a technical point of view the calculation in this paper consists of the evaluation of about 60 one-loop Feynman diagrams. The challenges of this task are due to the fact that these diagrams come with up to five external legs and three independent ratios of scales. In order to reduce the number of master integrals and to perform power expansions of the Feynman integrals, integration by parts methods and differential equation techniques will prove appropriate tools. They provide a general method to obtain higher powers of a Feynman integral once the leading power is given.

The paper is organized as follows: I define my notations in section 2. In section 3 I show how to get T^{II} at LO. In section 4 I present a method which uses differential equation techniques and allows for the extraction of higher powers of Feynman integrals once the leading power is given. Sections 5 is dedicated to the technical details of the calculation. After some remarks how to evaluate the Feynman diagrams occuring at NLO I show how to deal with meson wave functions at NLO. Especially the correct treatment of evancescent structures will be explained in detail. In section 6 the analytic results of the calculation will be given, whereas section 7 will provide the numerical analysis. I end up with the conclusions.

2 Notation and basic formulas

2.1 Kinematics

For the process $B \to \pi\pi$ we will assign the momenta p and q to the pions (fig. 2) which fulfil the condition

$$p^2, q^2 = 0. \tag{2}$$

This is the leading power approximation in $\Lambda_{\rm QCD}/m_b$. Let us define two Lorentz vectors n_+, n_- by:

$$n_+^\mu \equiv (1,0,0,1), \quad n_-^\mu \equiv (1,0,0,-1). \tag{3}$$

In the rest frame of the decaying meson p can be defined to be in the direction of n_+ and q to be in the direction of n_-. Light cone coordinates for the Lorentz vector z^μ are defined by:

$$z^+ \equiv \frac{z^0+z^3}{\sqrt{2}}, \quad z^- \equiv \frac{z^0-z^3}{\sqrt{2}}, \quad z_\perp \equiv (0, z^1, z^2, 0) \tag{4}$$

So one can decompose z^μ into:

$$z^\mu = \frac{z\cdot p}{p\cdot q} q^\mu + \frac{z\cdot q}{p\cdot q} p^\mu + z_\perp^\mu \tag{5}$$

such that

$$z_\perp \cdot p = z_\perp \cdot q = 0. \tag{6}$$

2.2 Colour factors

In our calculations we will use the following three colour factors, which arise from the SU(3) algebra:

$$C_N = \frac{1}{2}, \quad C_F = \frac{N_c^2-1}{2N_c} \quad \text{and} \quad C_G = N_c, \tag{7}$$

where $N_c = 3$ is the number of colours.

2.3 Meson wave functions

The pion light cone distribution amplitude ϕ_π is defined by

$$\langle \pi(p)|\bar q(z)_\alpha [\ldots] q'(0)_\beta |0\rangle_{z^2=0} = \frac{i f_\pi}{4} (\not p \gamma_5)_{\beta\alpha} \int_0^1 dx\, e^{ixp\cdot z} \phi_\pi(x). \tag{8}$$

The ellipsis $[\ldots]$ stands for the Wilson line

$$[z,0] = \mathrm{P} \exp\left(\int_0^1 dt\, i g_s z \cdot A(zt) \right), \tag{9}$$

which makes (8) gauge invariant. For the definition of the B-meson wave function ϕ_{B1} we need the special kinematics of the process. Following [2] let us define

$$\Psi_B^{\alpha\beta}(z,p_B) = \langle 0|\bar{q}_\beta(z)[\ldots]b_\alpha(0)|B(p_B)\rangle = \int \frac{d^4l}{(2\pi)^4} e^{-il\cdot z}\phi_B^{\alpha\beta}(l,p_B). \tag{10}$$

In the calculation of matrix elements we get terms like:

$$\int \frac{d^4l}{(2\pi)^4}\mathrm{tr}(\mathcal{A}(l)\phi_B(l)) = \int \frac{d^4l}{(2\pi)^4}\int d^4z\, e^{il\cdot z}\mathrm{tr}(\mathcal{A}(l)\Psi_B(z)). \tag{11}$$

We have to consider only the case that the amplitude $\mathcal{A}$ depends on l only through $l\cdot p$:

$$\mathcal{A} = \mathcal{A}(l\cdot p) \tag{12}$$

In this case we can use the B-meson wave function on the light cone which is given by [2]:

$$\begin{aligned}&\langle 0|\bar{q}_\alpha(z)[\ldots]b_\beta(0)|B(p_B)\rangle\Big|_{z^-,z_\perp=0} \qquad (13)\\ &\quad = -\frac{if_B}{4}[(\not{p}_B + m_b)\gamma_5]_{\beta\gamma}\int_0^1 d\xi\, e^{-i\xi p_B^- z^+}[\Phi_{B1}(\xi) + \not{n}_+\Phi_{B2}(\xi)]_{\gamma\alpha}\end{aligned}$$

where

$$\int_0^1 d\xi\,\Phi_{B1}(\xi) = 1 \quad \text{and} \quad \int_0^1 d\xi\,\Phi_{B2}(\xi) = 0. \tag{14}$$

It is now straightforward to write down the momentum projector of the B-meson:

$$\begin{aligned}&\int \frac{d^4l}{(2\pi)^4}\,\mathrm{tr}(A(2l\cdot p)\hat{\Psi}(l))\\ &\quad = \frac{-if_B}{4}\mathrm{tr}(\not{p}_B + m_B)\gamma_5\int_0^1 d\xi\,(\Phi_{B1}(\xi) + \not{n}_+\Phi_{B2}(\xi))A(\xi m_B^2)\end{aligned} \tag{15}$$

At this point we give the following definitions

$$\frac{m_B}{\lambda_B} \equiv \int_0^1 \frac{d\xi}{\xi}\phi_{B1}(\xi) \tag{16}$$

$$\lambda_n \equiv \frac{\lambda_B}{m_B}\int_0^1 \frac{d\xi}{\xi}\ln^n\xi\,\phi_{B1}(\xi). \tag{17}$$

3 Hard spectator interactions at LO

The effective weak Hamiltonian we deal with is given by [11]:

$$\mathcal{H}_{\text{eff}} = \frac{G_F}{\sqrt{2}}V_{ud}^*V_{ub}\,[C_1\mathcal{O}_1 + C_2\mathcal{O}_2] + \text{h.c.}, \tag{18}$$

where

$$\begin{aligned}\mathcal{O}_1 &= (\bar{d}p)_{V-A}(\bar{p}b)_{V-A},\\ \mathcal{O}_2 &= (\bar{d}_i p_j)_{V-A}(\bar{p}_j b_i)_{V-A}.\end{aligned} \tag{19}$$

Explicit expressions for the short-distance coefficients C_i can be obtained from [11]. The decay amplitude of $B \to \pi\pi$ is given by

$$\mathcal{A}(B \to \pi\pi) \equiv \langle \pi\pi | \mathcal{H}_{\rm eff} | B \rangle. \tag{20}$$

For later convenience we define

$$\mathcal{A}(B \to \pi\pi) \equiv \mathcal{A}(B \to \pi\pi)^{\rm I} + \mathcal{A}(B \to \pi\pi)^{\rm II} \tag{21}$$

where $\mathcal{A}^{\rm I}$ ($\mathcal{A}^{\rm II}$) belongs to the first (second) term of (1). Because $\mathcal{A}^{\rm I}$ and $\mathcal{A}^{\rm II}$ contain different hadronic quantities, the renormalisation scale dependence of both of them has to vanish separately. So we can set their scales to different values $\mu^{\rm I}$ and $\mu^{\rm II}$. As in $\mathcal{A}^{\rm I}$ there occurs only the mass scale m_b we can set $\mu^{\rm I} = m_b$. In $\mathcal{A}^{\rm II}$ there occurs also the hard-collinear scale $\sqrt{\Lambda_{\rm QCD} m_b}$. As we will see this scale is an appropriate choice for $\mu^{\rm II}$.

Because we only deal with the tree amplitude and do not consider penguin contractions only the matrix elements of the operators $\mathcal{O}_1$ and $\mathcal{O}_2$ are taken into account. These operators close under renormalisation such that the corresponding hard spectator amplitude is independent of the renormalisation scale.

The decay amplitudes of $B \to \pi\pi$ can be written in terms of a_i as follows [12]:

$$\begin{aligned}-\mathcal{A}(\bar{B}^0 \to \pi^+\pi^-) &= \left[\lambda'_u a_1 + \lambda'_p (a_4^p + r_\chi^\pi a_6^p)\right] A_{\pi\pi}\\ -\sqrt{2}\mathcal{A}(B^- \to \pi^-\pi^0) &= \lambda'_u (a_1 + a_2) A_{\pi\pi}\\ \mathcal{A}(\bar{B}^0 \to \pi^0\pi^0) &= \left[-\lambda'_u a_2 + \lambda'_p (a_4^p + r_\chi^\pi a_6^p)\right] A_{\pi\pi}\end{aligned} \tag{22}$$

where

$$A_{\pi\pi} = i\frac{G_F}{\sqrt{2}}(m_B^2 - m_\pi^2) f_+^{B\pi} f_\pi$$

and

$$r_\chi^\pi(\mu) = \frac{2m_\pi^2}{\bar{m}_b(\mu)(\bar{m}_u(\mu) + \bar{m}_d(\mu))}. \tag{23}$$

For the LO and NLO results of the a_i I refer to [12]. We define analogously to (21)

$$a_i = a_{i,\rm I} + a_{i,\rm II} \tag{24}$$

where the labels 'I' and 'II' refer to the contribution to $\mathcal{A}^{\rm I}$ and $\mathcal{A}^{\rm II}$.

The leading order of the hard spectator interactions which start at $\mathcal{O}(\alpha_s)$ is shown in fig. 2. The hard spectator scattering kernel $T^{\rm II}$, which does not depend on the wave functions, can be obtained by calculating the transition matrix element between free external quarks, to which we assign the momenta shown in fig. 2. The variables $x, \bar{x} \equiv 1-x, y, \bar{y} \equiv$

$1-y$ are the arguments of $T^{\rm II}$, which arise from the projection on the pion wave function (8). In the sense of power counting we count all components of l of $\mathcal{O}(\Lambda_{\rm QCD})$, while the components of p and q are $\mathcal{O}(m_b)$ or exactly zero. We define the following quantities

$$\xi \equiv \frac{l\cdot p}{p\cdot q}, \qquad \theta \equiv \frac{l\cdot q}{p\cdot q}. \tag{25}$$

We will see that in the end the dependence on θ vanishes in leading power such that we can use (15).

We consider the three cases $\bar{B}^0 \to \pi^+\pi^-$, $\bar{B}^0 \to \pi^0\pi^0$ and $B^- \to \pi^-\pi^0$. In the case, that the external quarks come with the flavour content of $\bar{B}^0 \to \pi^+\pi^-$, the LO hard spectator amplitude for the effective operator $\mathcal{O}_2$ reads:

$$\begin{aligned}
&A^{(1)}_{\rm spect.}(\bar{B}^0 \to \pi^+\pi^-) \equiv \\
&\quad \langle \bar{d}(\bar{x}p)u(xp)\,\bar{u}(\bar{y}q)d(yq)|\mathcal{O}_2|\bar{d}(l)b(p+q-l)\rangle_{\rm spect.} = \\
&\quad 4\pi\alpha_s C_F N_c \frac{1}{\bar{x}\xi m_B^2}\bar{d}(l)\gamma^\mu d(\bar{x}p)\,\bar{u}(xp)\gamma^\nu(1-\gamma_5)b(p+q-l) \\
&\quad \bar{d}(yq)\left(\frac{2\not{p}g_{\mu\nu}}{\bar{y}} - \frac{\not{p}}{y\bar{y}}\gamma_\mu\gamma_\nu\right)(1-\gamma_5)u(\bar{y}q),
\end{aligned} \tag{26}$$

where the quark antiquark states in the input and output channels of the matrix element form colour singlets. The subscript "spect." means that only diagrams with a hard spectator interaction are taken into account. The amplitude of $\mathcal{O}_1$ vanishes to this order in α_s. In the case of $\bar{B}^0 \to \pi^0\pi^0$ we get the tree amplitude from the matrix element of $\mathcal{O}_1$. The case $B^- \to \pi^-\pi^0$ does not need to be considered separately, because from isospin symmetry follows [13, 12]:

$$\sqrt{2}\mathcal{A}(B^- \to \pi^-\pi^0) = \mathcal{A}(\bar{B}^0 \to \pi^+\pi^-) + \mathcal{A}(\bar{B}^0 \to \pi^0\pi^0). \tag{27}$$

On the other hand the full amplitude is the convolution of $T^{\rm II}$ with the wave functions, given by (1). To extract $T^{\rm II}$ from (26) we need the wave functions with the same external states we have used in (26), i.e. we have to calculate the matrix elements (8) and (10), where the pion or B-meson states are replaced by free external quark states. To the order $\mathcal{O}(\alpha_s^0)$ we get

$$\begin{aligned}
\phi^{(0)}_{\pi^-\alpha\beta}(y') &\equiv \int d(z\cdot q)e^{-iz\cdot qy'}\langle \bar{u}(\bar{y}q)d(yq)|\bar{d}^i_\beta(z)u^i_\alpha(0)|0\rangle_{z^-,z_\perp=0} \\
&= 2\pi N_c\delta(y'-y)\bar{d}_\beta(yq)u_\alpha(\bar{y}q) \\
\phi^{(0)}_{\pi^+\alpha\beta}(x') &= 2\pi N_c\delta(x'-x)\bar{u}_\beta(xp)d_\alpha(\bar{x}p) \\
\phi^{(0)}_{B\alpha\beta}(l'^-) &\equiv \int dz^+ e^{il'^-z^+}\langle 0|\bar{d}_\beta(z)^i b_\alpha(0)^i|\bar{d}(l)b(p+q-l)\rangle_{z^-,z_\perp=0} \\
&= 2\pi N_c\delta(l'^- - l^-)\bar{d}_\beta(l)b_\alpha(p+q-l)
\end{aligned} \tag{28}$$

By using

$$A^{(1)}_{\text{spect.}} = \int dxdydl^- \, \phi^{(0)}_{\pi^+\alpha\alpha'}(x)\phi^{(0)}_{\pi^-\beta\beta'}(y)\phi^{(0)}_{B\gamma\gamma'}(l^-)T^{\text{II}(1)}(x,y,l^-)_{\alpha'\alpha\beta'\beta\gamma'\gamma} \tag{29}$$

we finally obtain:

$$\begin{aligned} T^{\text{II}(1)}(x,y,l^-)_{\alpha'\alpha\beta'\beta\gamma'\gamma} &= 4\pi\alpha_s \frac{C_F}{(2\pi)^3 N_c^2}\frac{1}{\xi\bar{x}m_B^2}\gamma^\mu_{\gamma'\alpha}\left[\gamma^\nu(1-\gamma_5)\right]_{\alpha'\gamma} \\ &\quad \left[\left(\frac{2\not{p}g_{\mu\nu}}{\bar{y}} - \frac{\not{p}}{y\bar{y}}\gamma_\mu\gamma_\nu\right)(1-\gamma_5)\right]_{\beta'\beta}. \end{aligned} \tag{30}$$

It should be noted that only the first summand of the above equation contributes after performing the Dirac trace in four dimensions. The second summand is evanescent. This will be important, when we will calculate the NLO corrections of the wave functions (see section 5.2).

If we plug the hadronic wave functions defined by (8) and (15) into (29) i.e. we calculate the matrix element (26) between meson states instead of free quark states, we get for the LO amplitude [2]:

$$A^{(1)}_{\text{spect.}} = -\frac{if_\pi^2 f_B C_F}{4N_c^2}4\pi\alpha_s \int_0^1 dxdyd\xi \, \Phi_{B1}(\xi)\phi_\pi(x)\phi_\pi(y)\frac{1}{\xi\bar{x}\bar{y}}. \tag{31}$$

Following (1) and the conventions of [3] we write our amplitude in the form:

$$A_{\text{spect.}i} = -im_B^2 \int_0^1 dxdyd\xi \, T_i^{\text{II}}(x,y,\xi) f_B \Phi_{B1}(\xi) f_\pi\phi_\pi(x) f_\pi\phi_\pi(y). \tag{32}$$

where in the case of $\bar{B} \to \pi^+\pi^-$ we define

$$\begin{aligned} A_{\text{spect.}1} &= \langle\mathcal{O}_2\rangle_{\text{spect.}} \\ A_{\text{spect.}2} &= \langle\mathcal{O}_1\rangle_{\text{spect.}} \end{aligned} \tag{33}$$

and in the case $\bar{B} \to \pi^0\pi^0$ we define

$$\begin{aligned} A_{\text{spect.}1} &= \langle\mathcal{O}_1\rangle_{\text{spect.}} \\ A_{\text{spect.}2} &= \langle\mathcal{O}_2\rangle_{\text{spect.}}. \end{aligned} \tag{34}$$

Because we use the NDR-scheme which preserves Fierz transformations for $\mathcal{O}_1$ and $\mathcal{O}_2$, T_i^{II} has the same form for both decay channels. From (31) and (32) we get:

$$\begin{aligned} T_1^{\text{II}(1)} &= 4\pi\alpha_s \frac{C_F}{4N_c^2}\frac{1}{\xi\bar{x}\bar{y}m_B^2} \\ T_2^{\text{II}(1)} &= 0 \quad . \end{aligned} \tag{35}$$

[2] $A_{\text{spect.}}$ is used for the matrix elements of the operators $\mathcal{O}_i$ between both free external quarks and hadronic meson states. It should become clear from the context what is actually meant.

4 Calculation of Feynman diagrams with differential equations

In this section I will discuss the extraction of subleading powers of Feynman integrals with the *method of differential equations* [14, 15, 16]. This method will prove to be easy to implement in a computer algebra system. The idea to obtain the analytic expansion of Feynman integrals by tracing them back to differential equations has first been proposed in [14]. This method, which is demonstrated in [14] by the one-loop two-point integral and in [15] by the two-loop sunrise diagram, uses differential equations with respect to the small or large parameter, in which the integral has to be expanded.

In contrast to [14, 15] I will discuss the case where setting the small parameter to zero gives rise to new divergences. In this case the initial condition is not given by the differential equation itself and also cannot be obtained by calculation of the simpler integral that is defined by setting the expansion parameter to zero. It is not possible to give a general proof, but it seems to be a rule, that one needs the leading power as a "boundary condition". An efficient way to calculate the leading power of Feynman integrals is provided by the *method of regions* [17, 18, 19, 20], whereas the subleading powers can be obtained from a differential equation. In the present section I will discuss which conditions the differential equation has to fulfil in order for this to work.

Although the examples I use below are taken from the present calculation, this method is very general and can be used in any case in which the expansion of Feynman integrals in small parameters is needed.

4.1 Description of the method

We start with a (scalar) integral of the form

$$I(p_1,\ldots,p_n,m_1,\ldots,m_n) = \int \frac{d^dk}{(2\pi)^d} \frac{1}{D_1\ldots D_n} \tag{36}$$

where the propagators are of the form $D_i = (k+p_i)^2 - m_i^2$. We assume that there is only one mass hierarchy, i.e. there are two masses $m \ll M$ such that all of the momenta and masses p_i and m_i are of $\mathcal{O}(m)$ or of $\mathcal{O}(M)$. We expand (36) in $\frac{m}{M}$ by replacing all small momenta and masses by $p_i \to \lambda p_i$ and expand in λ. After the expansion the bookkeeping parameter λ can be set to 1.

We obtain a differential equation for I by differentiating the integrand in (36) with respect to λ. This gives rise to new Feynman integrals with propagators of the form $\frac{1}{D_i^2}$ and scalar products $k \cdot p_i$ in the numerator. Those Feynman integrals, however, can be reduced to the original integral and to simpler integrals (i.e. integrals that contain less propagators in the denominator) by using integration by parts identities.

Finally we obtain for (36) a differential equation of the form

$$\frac{d}{d\lambda} I(\lambda) = h(\lambda) I(\lambda) + g(\lambda) \tag{37}$$

where $h(\lambda)$ contains only rational functions of λ and $g(\lambda)$ can be expressed by Feynman integrals with a reduced number of propagators. It is easy to see that h and g are unique if and only if I and the integrals contained in g are master integrals with respect to IBP-identities, i.e. they cannot be reduced to simpler integrals by IBP-identities. If $I(\lambda)$ is divergent in $\epsilon = \frac{4-d}{2}$, I, h and g have to be expanded in ϵ:

$$\begin{aligned} I &= \sum_i I_i \epsilon^i \\ h &= \sum_i h_i \epsilon^i \\ g &= \sum_i g_i \epsilon^i. \end{aligned} \tag{38}$$

Plugging (38) into (37) gives a system of differential equations for I_i, similar to (37). In the next paragraph we will consider an example for this case.

First let us assume that $h(\lambda)$ and $g(\lambda)$ have the following asymptotic behaviour in λ:

$$\begin{aligned} h(\lambda) &= h^{(0)} + \lambda h^{(1)} + \dots \\ g(\lambda) &= \sum_j \lambda^j g^{(j)}(\ln \lambda) \end{aligned} \tag{39}$$

i.e. h starts at λ^0, and we allow that g starts at a negative power of λ. We count $\ln \lambda$ as $\mathcal{O}(\lambda^0)$ so the $g^{(j)}$ may depend on $\ln \lambda$. This dependence, however, has to be such that

$$\lim_{\lambda \to 0} \lambda g^{(j)}(\ln \lambda) = 0. \tag{40}$$

The condition (40) is fulfilled, if the $g^{(j)}$ are of the form of a *finite* sum

$$\sum_{n=n_0}^{m} a_n \ln^n \lambda. \tag{41}$$

The limit $m \to \infty$ however can spoil the expansion (39). E.g. $e^{-\ln \lambda} = \frac{1}{\lambda}$ so the condition (40) is not fulfilled, which is due to the fact that we must not change the order of the limits $\lambda \to 0$ and $m \to \infty$.

Further we assume that also $I(\lambda)$ starts at λ^0

$$I(\lambda) = I^{(0)}(\ln \lambda) + \lambda I^{(1)}(\ln \lambda) + \dots \tag{42}$$

and plug this into (37) such that we obtain an equation which gives $I^{(i)}$ recursively:

$$\lambda^i I^{(i)} = \int_0^\lambda d\lambda' \lambda'^{i-1} \left(\sum_{j=0}^{i-1} h^{(j)} I^{(i-1-j)}(\ln \lambda') + g^{(i-1)}(\ln \lambda') \right). \tag{43}$$

I want to stress that, because h starts at $\mathcal{O}(\lambda^0)$, (43) is a recurrence relation, i.e. $I^{(j)}$ does not mix into $I^{(i)}$ if $j \geq i$. As the integral is only well defined if $i \geq 1$, we need the leading

power $I^{(0)}$ as "boundary condition" and (43) will give us all the higher powers in λ. It is easy to implement (43) in a computer algebra system, because we just need the integration of polynomials and finite powers of logarithms.

A modification is needed if h starts at λ^{-1} i.e.

$$h = -\frac{n}{\lambda} + h^{(0)} + \dots. \tag{44}$$

By replacing $\bar{I} \equiv \lambda^n I$ we obtain the differential equation

$$\frac{d}{d\lambda}\bar{I} = \left(\frac{n}{\lambda} + h\right)\bar{I} + \lambda^n g \tag{45}$$

which is similar to (37) and leads to

$$\lambda^{i+n} I^{(i)} = \int_0^\lambda d\lambda' \lambda'^{i+n-1} \left(\sum_{j=0}^{i+n-1} h^{(j)} I^{(i-1-j)}(\ln \lambda') + g^{(i-1)}(\ln \lambda') \right), \tag{46}$$

which is valid for $i \geq 1 - n$. So, if I starts at $\mathcal{O}(\lambda^{-n})$, the subleading powers result from the leading power.

4.2 Examples

We start with a pedagogic example:

Example 4.1.

$$I = \int \frac{d^d k}{(2\pi)^d} \frac{1}{k^2(k^2-\lambda)(k^2-1)} \tag{47}$$

where $\lambda \ll 1$. The exact expression for this integral is given by:

$$I = \frac{i}{(4\pi)^2} \frac{\ln \lambda}{1-\lambda} = \frac{i}{(4\pi)^2} \ln \lambda (1 + \lambda + \lambda^2 + \dots). \tag{48}$$

We see that I diverges for $\lambda \to 0$. As described e.g. in [20] we can obtain the leading power by expanding the integrand in the regions $k \sim \sqrt{\lambda}$ and $k \sim 1$. This leads in the first region to

$$\int \frac{d^d k}{(2\pi)^d} \frac{-1}{k^2(k^2-\lambda)} = -\frac{i}{(4\pi)^{2-\epsilon}} \Gamma(1+\epsilon) \left(\frac{1}{\epsilon} + 1 - \ln \lambda\right) \tag{49}$$

and in the second region to

$$\int \frac{d^d k}{(2\pi)^d} \frac{1}{k^4(k^2-1)} = \frac{i}{(4\pi)^{2-\epsilon}} \Gamma(1+\epsilon) \left(\frac{1}{\epsilon} + 1\right) \tag{50}$$

such that we finally obtain

$$I^{(0)}(\ln \lambda) = \frac{i}{(4\pi)^2} \ln \lambda. \tag{51}$$

This is the result we obtain from the leading power of (48). We write the derivative of I with respect to λ in the following form:

$$\frac{d}{d\lambda}I = \frac{1}{1-\lambda}\left[I - \int \frac{d^dk}{(2\pi)^d}\frac{1}{k^2(k^2-\lambda)^2}\right]. \tag{52}$$

We obtained the right hand side of (52) by decomposing $\frac{d}{d\lambda}I$ into partial fractions. Of course this decomposition is not unique which is due to the fact that I itself is not a master integral but can be further simplified by partial fractioning. From (52) and (37) we get:

$$\begin{aligned} h &= \frac{1}{1-\lambda} = 1 + \lambda + \lambda^2 + \ldots \\ g &= \frac{i}{(4\pi)^2}\frac{1}{\lambda(1-\lambda)} = \frac{i}{(4\pi)^2}\left(\lambda^{-1} + 1 + \lambda + \ldots\right) \end{aligned} \tag{53}$$

such that the coefficients in the expansion in λ according to (39) do not depend on the power label (k):

$$h^{(k)} = 1 \quad \text{and} \quad g^{(k)} = \frac{i}{(4\pi)^2}. \tag{54}$$

We obtain for the recurrence relation (43):

$$I^{(k)} = \frac{1}{\lambda^k}\int_0^\lambda d\lambda'\,\lambda'^{k-1}\left(\sum_{j=0}^{k-1} I^{(k-1-j)}(\ln\lambda') + \frac{i}{(4\pi)^2}\right). \tag{55}$$

Using the initial value (51) it is easy to prove by induction

$$I^{(k)}(\ln\lambda) = \frac{i}{(4\pi)^2}\ln\lambda \quad \forall k \geq 0. \tag{56}$$

This result coincides with (48).

The first nontrivial example, we want to consider, is the following three-point integral:

Example 4.2.

$$I = \int \frac{d^dk}{(2\pi)^d}\frac{1}{k^2(k+un_- + l)^2(k+n_+ + n_-)^2}. \tag{57}$$

Here n_+ and n_- are collinear Lorentz vectors, which fulfil $n_+^2 = n_-^2 = 0$ and $n_+ \cdot n_- = \frac{1}{2}$, u is a real number between 0 and 1 and l is a Lorentz vector with $l^2 = 0$ and $l^\mu \ll 1$. Furthermore we define

$$\xi = 2l \cdot n_+ \quad \text{and} \quad \theta = 2l \cdot n_-. \tag{58}$$

We expand I in l, so we make the replacement $l \to \lambda l$ and differentiate I with respect to λ. The integral is not divergent in ϵ such that we obtain a differential equation of the form (37) where the Taylor series of $h(\lambda)$ starts at λ^0 as in (39). In $g(\lambda)$ only two-point integrals

occur, which are easy to calculate. I do not want to give the explicit expressions for h and g because they are complicated, their exact form is not needed to understand this example and they can be handled by a computer algebra system. Because the leading power of I is of $\mathcal{O}(\lambda^0)$, (43) gives all of the subleading powers.

We obtain the leading power as follows: First we have to identify the regions, which contribute at leading power. If we decompose k into

$$k^\mu = 2k \cdot n_+ n_-^\mu + 2k \cdot n_- n_+^\mu + k_\perp^\mu \tag{59}$$

we note that the only regions, which remain at leading power, are the hard region $k^\mu \sim 1$ and the hard-collinear region

$$\begin{aligned} k \cdot n_+ &\sim 1 \\ k \cdot n_- &\sim \lambda \\ k_\perp^\mu &\sim \sqrt{\lambda}. \end{aligned} \tag{60}$$

The soft region $k^\mu \sim \lambda$ leads at leading power to a scaleless integral, which vanishes in dimensional regularisation. In the hard region we expand the integrand to

$$\frac{1}{k^2(k+un_-)^2(k+n_++n_-)^2}. \tag{61}$$

By introducing a convenient Feynman parametrisation we obtain for the $(4-2\epsilon)$-dimensional integral over (61):

$$\frac{i}{(4\pi)^{2-\epsilon}}\Gamma(1+\epsilon)\exp(i\pi\epsilon)\frac{1}{u}\left(\frac{\ln(1-u)}{\epsilon} - \frac{1}{2}\ln^2(1-u)\right). \tag{62}$$

In the hard-collinear region we expand the integrand to

$$\frac{1}{k^2(k+un_-+\theta n_+)^2(2k\cdot n_++1)}. \tag{63}$$

The integral over (63) gives:

$$\begin{aligned} \frac{i}{(4\pi)^{2-\epsilon}}\Gamma(1+\epsilon)\exp(i\pi\epsilon)\frac{1}{u}\Bigg(&\frac{-\ln(1-u)}{\epsilon} + 2\mathrm{Li}_2(u) + \frac{1}{2}\ln^2(1-u) \\ &+ \ln u \ln(1-u) + \ln(1-u)\ln\theta\Bigg). \end{aligned} \tag{64}$$

Adding (62) and (64) together we get the leading power of (57):

$$I^{(0)} = \frac{i}{(4\pi)^2}\frac{1}{u}\left(2\mathrm{Li}_2(u) + \ln u \ln(1-u) + \ln(1-u)\ln\theta\right). \tag{65}$$

By plugging (65) into (43) we obtain I at $\mathcal{O}(\lambda)$:

$$
\begin{aligned}
&I^{(1)} = \\
&\frac{i}{(4\pi)^2}\frac{1}{u}\Bigg[\theta\Bigg(-2+\ln u+\frac{\ln(1-u)\ln\theta}{u}+\frac{\ln(1-u)\ln u}{u}+\ln\xi+\frac{2\mathrm{Li}_2(u)}{u}\Bigg)- \\
&\qquad\xi\Bigg(\frac{\ln u}{1-u}+2\frac{\ln(1-u)}{u}+\frac{\ln(1-u)\ln\theta}{u}+\frac{\ln(1-u)\ln u}{u}+ \\
&\qquad\frac{\ln\xi}{1-u}+\frac{2\mathrm{Li}_2(u)}{u}\Bigg)\Bigg].
\end{aligned}
\tag{66}
$$

Now we want to consider the following four-point integral

Example 4.3.

$$
I=\int\frac{d^dk}{(2\pi)^d}\frac{1}{k^2(k+n_-)^2(k+l-n_+)^2(k+l-un_+)^2},
\tag{67}
$$

where we used the same variables, which were introduced in (57). This example is very special, because in this case our method will allow us to obtain not only the subleading but also the leading power in l. I is divergent in ϵ such that we obtain after the expansion (38) a system of differential equations of the following form:

$$
\begin{aligned}
\frac{d}{d\lambda}I_{-1} &= h_0 I_{-1}+g_{-1} \\
\frac{d}{d\lambda}I_0 &= h_0 I_0+h_1 I_{-1}+g_0.
\end{aligned}
\tag{68}
$$

It turns out that in our example h takes the simple form

$$
h=-\frac{2+2\epsilon}{\lambda}
\tag{69}
$$

such that analogously to (45) we can transform (68) into

$$
\begin{aligned}
\frac{d}{d\lambda}(\lambda^2 I_{-1}) &= \lambda^2 g_{-1} \\
\frac{d}{d\lambda}(\lambda^2 I_0) &= -2\lambda I_{-1}+\lambda^2 g_0.
\end{aligned}
\tag{70}
$$

This system of differential equations can easily be integrated to:

$$
\begin{aligned}
I_{-1}^{(i)} &= \frac{1}{\lambda^{i+2}}\int_0^\lambda d\lambda'\,\lambda'^{i+1}g_{-1}^{(i-1)} \\
I_0^{(i)} &= \frac{1}{\lambda^{i+2}}\int_0^\lambda d\lambda'\,\lambda'^{i+1}\left(-2I_{-1}^{(i)}+g_0^{(i-1)}\right)
\end{aligned}
\tag{71}
$$

where the superscript (i) denotes the order in λ as in (39) and (42). Both I_{-1} and I_0 start at $\mathcal{O}(\lambda^{-1})$. Because (71) is valid for $i \geq -1$, it gives us the leading power expression, which reads:

$$I^{(-1)} = \frac{i}{(4\pi)^{2-\epsilon}}\Gamma(1+\epsilon)\frac{2}{u\xi}\left(\frac{1}{\epsilon} - 1 - \frac{\ln u}{1-u} - \ln\xi\right) \tag{72}$$

where $\xi = 2l \cdot n_+$ as in the example above. The exact expression for (67) can be obtained from [21]. Thereby (72) can be tested.

In the last paragraph I want to return to Example 4.2. I will show how we can use differential equations to prove that the integral (57) depends in leading power only on the soft kinematical variable $\theta = 2l \cdot n_-$ and not on $\xi = 2l \cdot n_+$. We need derivatives of the integral with respect to ξ and θ, which we have to express through derivatives with respect to l^μ. These derivatives can be applied directly to the integrand, whose dependence on l^μ is obvious. We start from the following equations:

$$\begin{aligned} n_+^\mu \frac{\partial}{\partial l^\mu} I &= \frac{\partial}{\partial\theta} I + \xi \frac{\partial}{\partial l^2} I \\ n_-^\mu \frac{\partial}{\partial l^\mu} I &= \frac{\partial}{\partial\xi} I + \theta \frac{\partial}{\partial l^2} I \\ l^\mu \frac{\partial}{\partial l^\mu} I &= \xi \frac{\partial}{\partial\xi} I + \theta \frac{\partial}{\partial\theta} I + 2l^2 \frac{\partial}{\partial l^2} I \end{aligned} \tag{73}$$

which lead to

$$\begin{aligned} \xi \frac{\partial}{\partial\xi} I &= \frac{1}{2}(-\theta n_+^\mu + \xi n_-^\mu + l^\mu)\frac{\partial}{\partial l^\mu} I \\ \theta \frac{\partial}{\partial\theta} I &= \frac{1}{2}(\theta n_+^\mu - \xi n_-^\mu + l^\mu)\frac{\partial}{\partial l^\mu} I. \end{aligned} \tag{74}$$

where we have set $l^2 = 0$ in (74). Using (74) we can show that in leading power (57) depends only on θ and not on ξ. So we can simplify the calculation of the leading power by making the replacement $l^\mu \to \theta n_+^\mu$. The proof goes as follows: From (42) we see that the statement "$I^{(0)}$ does not depend on ξ" is equivalent to

$$\xi \frac{\partial}{\partial\xi} I(\xi\lambda, \theta\lambda) = \mathcal{O}(\lambda). \tag{75}$$

Using the first equation of (74) we get

$$\xi \frac{\partial}{\partial\xi} I(\xi\lambda, \theta\lambda) = \mathcal{O}(\lambda) I(\xi\lambda, \theta\lambda) + \mathcal{O}(\lambda). \tag{76}$$

Because we know (e.g. from power counting) that $I(\xi\lambda, \theta\lambda)$ starts at λ^0, (75) is proven.

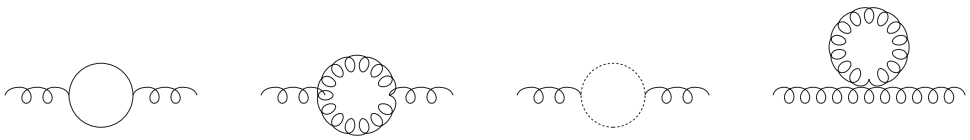

Figure 3: Gluon self energy

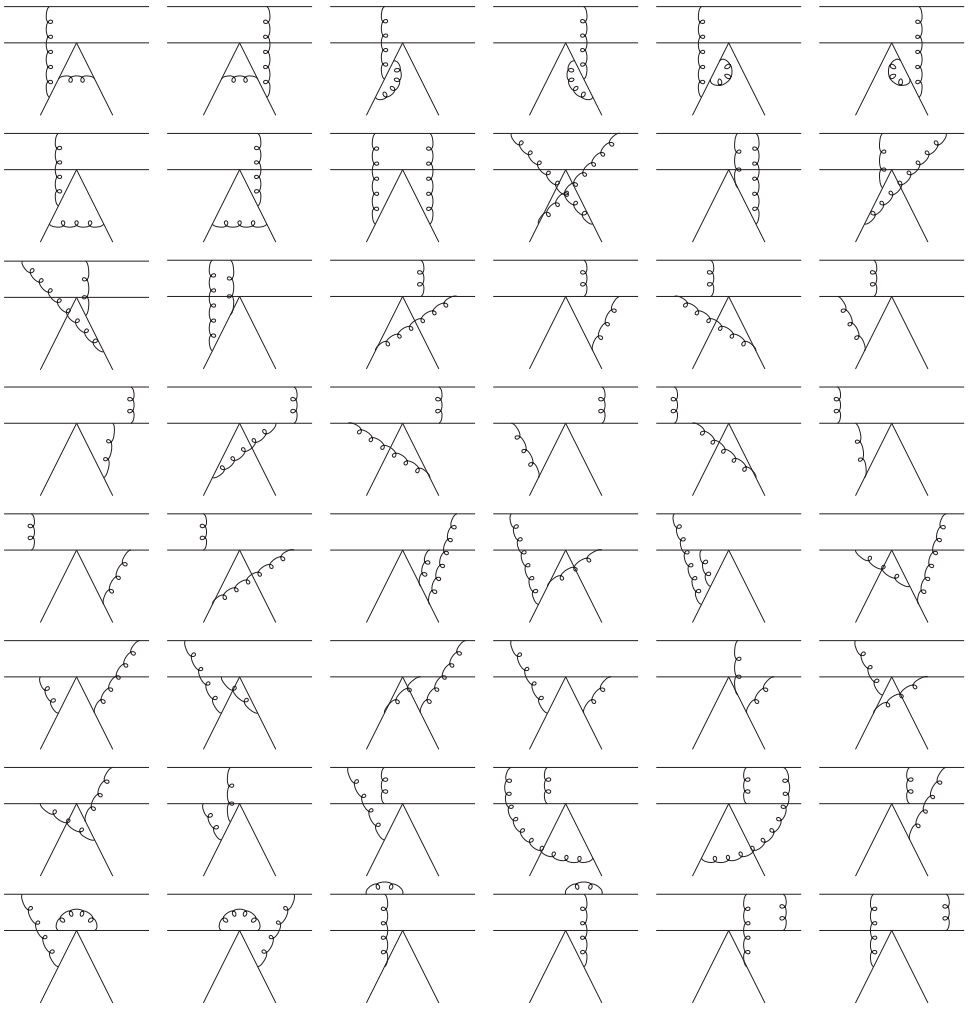

Figure 4: Abelian diagrams

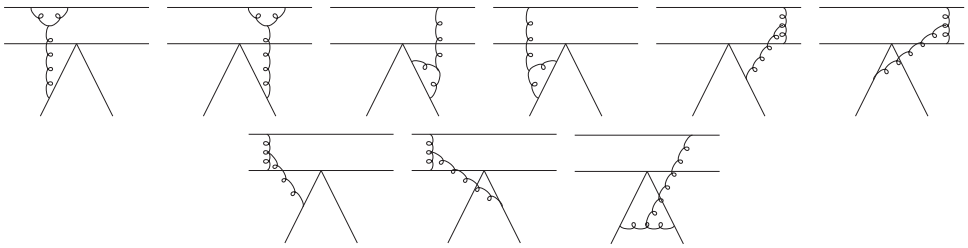

Figure 5: Nonabelian diagrams

5 Technical details of the NLO calculation

5.1 Evaluation of the Feynman diagrams

The diagrams that contribute to $T_1^{\rm II}$ at NLO are listed in fig. 3 - 5. The diagrams are evaluated in leading power in $\Lambda_{\rm QCD}/m_b$. We do not use an effective theory like SCET but evaluate the diagrams in full QCD using free external quark states, to which we assign the momenta given in fig. 2. The Feynman integrals have to be evaluated in leading power in $\Lambda_{\rm QCD}/m_b$. After reducing the number of Feynman integrals by integration by parts (IBP) identities [22, 23], we get the leading power of the master integrals using the method of regions (see e.g. [20]). In many cases the method of regions allows for a further reduction of master integrals. E.g. the first diagrams in the second line of fig. 5 comes with the scalar integral

$$\int \frac{d^dk}{(2\pi)^d} \frac{1}{k^2(k+\bar{x}p-l)^2(k+\bar{x}p+\bar{y}q-l)^2((k+p+q-l)^2-m_b^2)}. \tag{77}$$

This integral can be calculated in leading power by setting $\theta = 0$, i.e. we make the replacement $l^\mu \to \xi q^\mu$ where ξ and θ are defined in (25). This can be seen as follows: Counting soft momenta as $\mathcal{O}(\lambda)$ and hard momenta as $\mathcal{O}(m_b)$ the regions of space where (77) gives a leading power contribution are

$$\begin{aligned} &k^\mu \sim m_b \\ &k^\mu \sim \lambda \\ &k\cdot p \sim \lambda \quad k_\perp^\mu \sim \sqrt{\lambda} \quad k\cdot q \sim m_b. \end{aligned}$$

In these regions l^μ occurs only in the combination $l \cdot p$. So we can make the replacement $l^\mu \to \xi q^\mu$. It can be easily seen that this replacement allows to reduce (77) to three-point functions by decomposing the integrand into partial fractions. Alternatively one can use the exact expression (137) for the four-point integral with one massive propagator line, which is given in appendix A. After taking the leading power it can easily be seen that we get the same result as by just making the replacement $l^\mu \to \xi q^\mu$.

Tensor integrals of the form $\int \frac{d^dk}{(2\pi)^d}(k^\mu, k^\mu k^\nu, ...)/\text{Denominator}$ can be reduced to scalar integrals using the methods of [24]. This reduction may make it necessary to calculate

subleading powers of Feynman integrals to obtain some diagrams in leading power. Furthermore, subleading powers of Feynman integrals are necessary in some diagrams, where the leading power vanishes because of the equations of motion. The methods of the last section, however, allow for an extraction of the subleading powers once the leading powers have been calculated.

It is instructive and helps to avoid mistakes to obtain the Feynman integrals in two independent ways. Instead of using arguments depending on power counting we can obtain the power expansion of the integrals by calculating the exact integrals and expanding the results. The exact expressions of massless four-point integrals are given in [21]. Quite general expressions for four-point integrals with one massive propagator are given in appendix A. All of the integrals that were used for the present calculation have passed this independent test.

5.2 Wavefunction contributions

5.2.1 General remarks

It has already been demonstrated in section 3 how in principle we can extract the scattering kernel T^{II} of (1) from the amplitude if we know the wave functions. T^{II} does not depend on the hadronic physics and on the form of the wave function ϕ_π and ϕ_B in particular, so we can get T^{II} by calculating the matrix elements of the effective operators between free quark states carrying the momenta shown in fig. 2 on page 3. Because we calculate T^{II} in NLO we need unlike as in section 3 the wave functions up to NLO. Let us write the second term of (1) in the following formal way:

$$\mathcal{A}_{\text{spect.}} = \phi_\pi \otimes \phi_\pi \otimes \phi_B \otimes T^{\mathrm{II}}. \tag{78}$$

All of the objects arising in (78) have their perturbative series in α_s, so (78) becomes

$$\begin{aligned}
\mathcal{A}^{(1)}_{\text{spect.}} &= \phi_\pi^{(0)} \otimes \phi_\pi^{(0)} \otimes \phi_B^{(0)} \otimes T^{\mathrm{II}(1)} \\
\mathcal{A}^{(2)}_{\text{spect.}} &= \phi_\pi^{(1)} \otimes \phi_\pi^{(0)} \otimes \phi_B^{(0)} \otimes T^{\mathrm{II}(1)} + \phi_\pi^{(0)} \otimes \phi_\pi^{(1)} \otimes \phi_B^{(0)} \otimes T^{\mathrm{II}(1)} + \\
&\quad \phi_\pi^{(0)} \otimes \phi_\pi^{(0)} \otimes \phi_B^{(1)} \otimes T^{\mathrm{II}(1)} + \phi_\pi^{(0)} \otimes \phi_\pi^{(0)} \otimes \phi_B^{(0)} \otimes T^{\mathrm{II}(2)} \\
&\quad \vdots
\end{aligned} \tag{79}$$

where the superscript (i) denotes the order[3] in α_s. In order to get $T^{\mathrm{II}(2)}$ we have to calculate $\mathcal{A}^{(2)}_{\text{spect.}}$, $\phi_\pi^{(1)}$ and $\phi_B^{(1)}$ for our final states. Then $T^{\mathrm{II}(2)}$ is given by

$$\begin{aligned}
&\phi_\pi^{(0)} \otimes \phi_\pi^{(0)} \otimes \phi_B^{(0)} \otimes T^{\mathrm{II}(2)} = \\
&\quad \mathcal{A}^{(2)}_{\text{spect.}} - \phi_\pi^{(1)} \otimes \phi_\pi^{(0)} \otimes \phi_B^{(0)} \otimes T^{\mathrm{II}(1)} - \phi_\pi^{(0)} \otimes \phi_\pi^{(1)} \otimes \phi_B^{(0)} \otimes T^{\mathrm{II}(1)} - \\
&\quad \phi_\pi^{(0)} \otimes \phi_\pi^{(0)} \otimes \phi_B^{(1)} \otimes T^{\mathrm{II}(1)}
\end{aligned} \tag{80}$$

[3] Note that the hard spectator scattering kernel starts at $\mathcal{O}(\alpha_s)$. So we call $T^{\mathrm{II}(1)}$ the LO and $T^{\mathrm{II}(2)}$ the NLO.

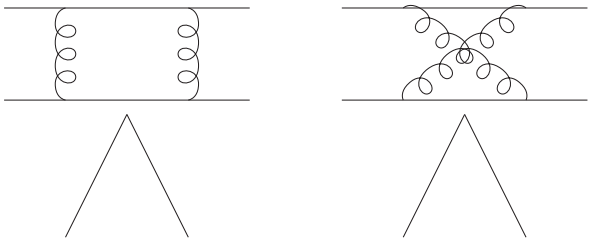

Figure 6: Example for diagrams which obviously belong to the form factor

At this point a subtlety occurs. Let us have a closer look to the factorization formula (1). By calculating the first order in α_s of the partonic form factor $F^{B\to\pi,(1)}$, which is defined by free quark states instead of hadronic external states, we see that it can be written in the form

$$F^{B\to\pi,(1)} = \phi_\pi^{(0)} \otimes \phi_B^{(0)} \otimes T^{(1)}_{\text{formfact.}}. \tag{81}$$

But $T^{(1)}_{\text{formfact.}}$ is not part of T^{II}. So we have to modify (80) insofar as we have to subtract the right hand side of (81) from the right hand side of (80):

$$\begin{aligned}
&\phi_\pi^{(0)} \otimes \phi_\pi^{(0)} \otimes \phi_B^{(0)} \otimes T^{\text{II}(2)} = \\
&\quad \mathcal{A}^{(2)}_{\text{spect.}} - \phi_\pi^{(1)} \otimes \phi_\pi^{(0)} \otimes \phi_B^{(0)} \otimes T^{\text{II}(1)} - \phi_\pi^{(0)} \otimes \phi_\pi^{(1)} \otimes \phi_B^{(0)} \otimes T^{\text{II}(1)} - \\
&\quad \phi_\pi^{(0)} \otimes \phi_\pi^{(0)} \otimes \phi_B^{(1)} \otimes T^{\text{II}(1)} - \phi_\pi^{(0)} \otimes \phi_\pi^{(0)} \otimes \phi_B^{(0)} \otimes T^{(1)}_{\text{formfact.}} \otimes T^{\text{I}(1)}
\end{aligned} \tag{82}$$

In (82) we did not include the term $F^{B\to\pi,(2)} \otimes T^{\text{I}(0)}$, because it is obviously identical with the diagrams where the gluons do not interact with the emitted pion (e.g. those of fig. 6). Those diagrams where not considered in the last section. So we do not have to consider them here.

The wave functions for free external quark states are given at LO by (28). At NLO there exist three possible contractions: The two external quark states can be connected by a gluon propagator or one of the external quarks can be connected to the eikonal Wilson line of the wave function (fig. 7). The diagrams of fig. 7(a),(b) and (c) give the order α_s of the "pion wave function for free quarks", i.e. we have replaced the pion final state $\langle\pi(p)|$ in (8) by the free quark state $\langle\bar{q}'(\bar{x}p)q(xp)|$. The Fourier transformed wave function $\phi_\pi^{(1)}(x')$ is defined analogously to (28). For the diagrams in fig. 7 (a), (b) and (c) respectively we get:

$$\begin{aligned}
\phi^{(\text{a}),(1)}_{\pi\alpha\beta}(x') &= 8\pi^2 i\alpha_s C_F N_c \int \frac{d^dk}{(2\pi)^d} \frac{\delta(x'-x-\frac{k^+}{p^+}) - \delta(x'-x)}{k^2k^+} \bar{q}_\beta(xp) \left[\frac{1}{\not k - \bar{x}\not p}\gamma^+ q'(\bar{x}p)\right]_\alpha \\
\phi^{(\text{b}),(1)}_{\pi\alpha\beta}(x') &= 8\pi^2 i\alpha_s C_F N_c \int \frac{d^dk}{(2\pi)^d} \frac{\delta(x-x'-\frac{k^+}{p^+}) - \delta(x-x')}{k^2k^+} \left[\bar{q}(xp)\gamma^+ \frac{1}{\not k - x\not p}\right]_\beta q'_\alpha(\bar{x}p)
\end{aligned}$$

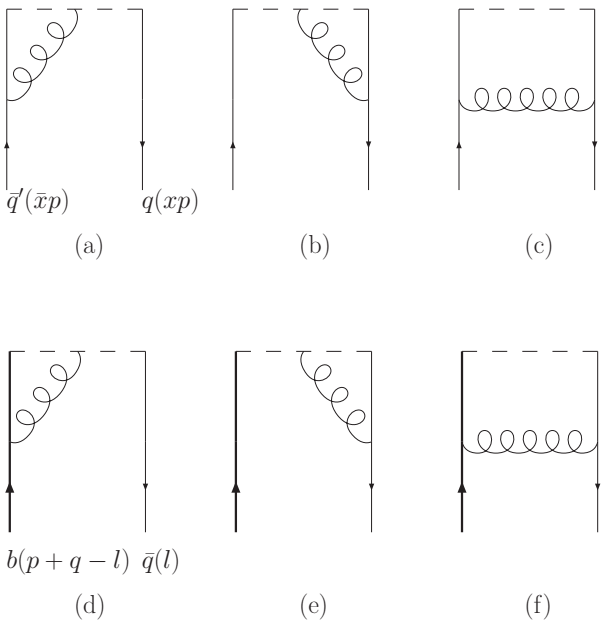

Figure 7: NLO contributions to the meson wave functions. The dashed line stands for the eikonal Wilson line which makes the wave functions gauge invariant.

$$\phi^{(c),(1)}_{\pi\alpha\beta}(x') = 8\pi^2 i\alpha_s C_F N_c \int \frac{d^dk}{(2\pi)^d} \frac{\delta(x'-x+\frac{k^+}{p^+})}{k^2} \left[\bar{q}(xp)\gamma^\tau \frac{1}{x\not{p}-\not{k}}\right]_\beta \left[\frac{1}{\not{k}+\bar{x}\not{p}}\gamma_\tau q'(\bar{x}p)\right]_\alpha \tag{83}$$

5.2.2 Evanescent operators

At NLO the convolution of the wave functions with the tree level kernel $T^{\mathrm{II},(1)}$ gives rise to new Dirac structures, which, however, can in four dimensions be reduced to the tree level Dirac structures. So we obtain the tree level Dirac structures plus further evanescent structures, which vanish for $d = 4$ but give finite contributions if they are multiplied by UV-poles. We define our renormalisation scheme such that we subtract the UV-poles and these finite parts of the evanescent structures.

The tree level kernel (30) contains two Dirac structures where the second one is evanescent (after the the projection on the wave functions). We write $T^{\mathrm{II}(1)}$ in the following form:

$$T^{\mathrm{II}(1)}(x,y,l^-) \equiv \frac{1}{\bar{x}l^-}\gamma^\mu \tilde{\otimes} \gamma^\nu (1-\gamma_5) \otimes \left(\frac{2\not{p}g_{\mu\nu}}{\bar{y}} - \frac{\not{p}\gamma_\mu\gamma_\nu}{y\bar{y}}\right)(1-\gamma_5) \tag{84}$$

where the symbol $\tilde{\otimes}$ stands for the "wrong contraction" of the Dirac indices i.e. the Dirac indices are given by

$$\left[\Gamma^1 \tilde{\otimes} \Gamma^2 \otimes \Gamma^3\right]_{\alpha'\alpha\beta'\beta\gamma'\gamma} = \Gamma^1_{\gamma'\alpha}\Gamma^2_{\alpha'\gamma}\Gamma^3_{\beta'\beta} \tag{85}$$

as in (30). The "right contraction" is defined by the symbol $\otimes$ i.e. writing the Dirac indices explicitly

$$\left[\Gamma^1 \otimes \Gamma^2 \otimes \Gamma^3\right]_{\alpha'\alpha\beta'\beta\gamma'\gamma} = \Gamma^1_{\alpha'\alpha}\Gamma^2_{\gamma'\gamma}\Gamma^3_{\beta'\beta}. \tag{86}$$

In $d = 4$ the wrong and the right contraction are related by Fierz transformations. It is convenient and commonly used to define the renormalised wave functions in terms of the right contraction, i.e. to define $\phi_\pi^{\text{ren.}}$ by renormalising the operator $\bar{q}(z)\gamma^\mu\gamma_5 q'(0)$ instead of $\bar{q}(z)_\beta q'(0)_\alpha$. This is why we define our renormalisation scheme such that only the UV-finite part of the right contraction operators remains: Using the notation of (84) – (86) we define the following operators:

$$\mathcal{O}_0(x,y,l^-) \equiv -\frac{1}{2l^-\bar{x}}\gamma^\mu(1-\gamma_5)\otimes\gamma_\mu(1-\gamma_5)\otimes\frac{2\not{p}}{\bar{y}}(1-\gamma_5) \tag{87}$$

$$\mathcal{O}_1(x,y,l^-) \equiv \frac{1}{l^-\bar{x}}\gamma^\mu\tilde{\otimes}\gamma_\mu(1-\gamma_5)\otimes\frac{2\not{p}}{\bar{y}}(1-\gamma_5) \tag{88}$$

$$\mathcal{O}_2(x,y,l^-) \equiv \frac{1}{l^-\bar{x}}\gamma^\mu\tilde{\otimes}\gamma^\nu(1-\gamma_5)\otimes\frac{-\not{p}\gamma_\mu\gamma_\nu}{y\bar{y}}(1-\gamma_5). \tag{89}$$

The matrix elements of these operators are defined analogously to (29):

$$\langle\mathcal{O}_i\rangle \equiv \int dx'dy'dl'^-\,\phi_{\pi\alpha\alpha'}(x')\phi_{\pi\beta\beta'}(y')\phi_{B\gamma\gamma'}(l'^-)\mathcal{O}_{i\,\alpha'\alpha\beta'\beta\gamma'\gamma}(x',y',l'^-). \tag{90}$$

Note that $\langle\mathcal{O}_1+\mathcal{O}_2\rangle$ is just the convolution of the tree level kernel (84) with the wave functions. Furthermore by using Fierz identities it is easy to prove that we have in four dimensions

$$\langle\mathcal{O}_0\rangle = \langle\mathcal{O}_1\rangle \tag{91}$$

$$\langle\mathcal{O}_2\rangle = 0. \tag{92}$$

So we define the following evanescent operators:

$$E_1 \equiv \mathcal{O}_2 \tag{93}$$

$$E_2 \equiv \mathcal{O}_1 - \mathcal{O}_0 \tag{94}$$

$$E_3 \equiv \frac{1}{\bar{x}\bar{y}l^-}\left(\gamma^\mu\gamma^\nu\gamma^\rho\tilde{\otimes}\gamma_\rho\gamma_\nu\gamma_\mu(1-\gamma_5)+\frac{(2-d)^2}{2}\gamma^\mu(1-\gamma_5)\otimes\gamma_\mu(1-\gamma_5)\right) \otimes 2\not{p}(1-\gamma_5) \tag{95}$$

$$E_4 \equiv \frac{1}{\bar{x}y\bar{y}l^-}\gamma^\mu\gamma^\lambda\gamma^\tau\tilde{\otimes}\gamma_\tau\gamma_\lambda\gamma^\nu(1-\gamma_5)\otimes\not{p}\gamma_\mu\gamma_\nu(1-\gamma_5) \tag{96}$$

where we have defined E_3 and E_4 for later convenience. Using those operator definitions we define our renormalisation scheme such that we subtract the UV-pole of $\langle\mathcal{O}_0\rangle$ and the finite parts of $\langle E_i\rangle$ i.e. terms of the form $\frac{1}{\epsilon_{\text{UV}}}\langle E\rangle$, where $\langle E\rangle$ is an arbitrary evanescent structure. It is important to note that we do not subtract IR-poles, because they depend not only on

the operator but also on the external states the operator is sandwiched in between. They have to vanish in (82) such that the hard scattering kernel is finite. Finally we obtain the same result as if we had regularised the IR-divergences by small quark and gluon masses because the evanescent structures vanish in $d = 4$. The renormalisation scheme defined above is the same scheme that was used in [3].

In the next step we will calculate the convolution integral of $T^{\mathrm{II},(1)}$ with the NLO wave functions given by (83), i.e. we have to calculate the renormalised matrix elements of $\mathcal{O}_1 + \mathcal{O}_2$ at NLO.

5.2.3 Wave function of the emitted pion

First we consider the renormalisation of the emitted pion wave function: Because the contribution of the wave functions $\phi_\pi^{(a)}$ and $\phi_\pi^{(b)}$ does not change the Dirac structure of the operators, we do not need to consider evanescent operators when we calculate the diagrams of fig. 7(a),(b). So for the emitted pion wave function these diagrams give after renormalisation:

$$\begin{aligned}\langle \mathcal{O}_1^{\text{ren.}} + \mathcal{O}_2^{\text{ren.}} \rangle_{\text{emitted}}^{(1),(\text{a}),(\text{b})} = \frac{2\alpha_s}{4\pi} C_F \Bigg[\left(-\frac{1}{\epsilon_{\text{IR}}} + 2 \ln \frac{\mu_{\text{UV}}}{\mu_{\text{IR}}} \right) \frac{\ln \bar{y} + 2y}{y} \langle \mathcal{O}_1 \rangle^{(0)} \\ - \left(\frac{1}{\epsilon_{\text{IR}}} + 2 \ln \mu_{\text{IR}} \right) (2 + \ln y + \ln \bar{y}) \langle \mathcal{O}_2 \rangle^{(0)} \Bigg] \end{aligned} \tag{97}$$

where the LO matrix elements $\langle \mathcal{O}_i \rangle^{(0)}$ can be obtained from (26). Note that we kept the IR-pole times the evanescent matrix element $\langle \mathcal{O}_2 \rangle^{(0)}$. This is needed for consistency because we also kept similar terms in the QCD-calculation of $\mathcal{A}_{\text{spect.}}$. Furthermore it allows us to show that all IR-divergences vanish.

The diagram in fig. 7(c) mixes different Dirac structures. So we have to include evanescent operators in the renormalisation. In the case of the emitted pion wave function the operator $\mathcal{O}_1$ does not mix under renormalisation with the evanescent operator E_1 (93). We obtain for the renormalised matrix element:

$$\langle \mathcal{O}_1^{\text{ren.}} \rangle_{\text{emitted}}^{(1),(\text{c})} = -\frac{2\alpha_s}{4\pi} C_F \frac{\bar{y} \ln \bar{y}}{y} \left(-\frac{1}{\epsilon_{\text{IR}}} + 2 \ln \frac{\mu_{\text{UV}}}{\mu_{\text{IR}}} \right) \langle \mathcal{O}_1 \rangle^{(0)}. \tag{98}$$

The matrix element of E_1 however has an overlap with $\mathcal{O}_1$:

$$\begin{aligned}\langle E_1 \rangle_{\text{emitted}}^{(1),(\text{c})} = \frac{\alpha_s}{4\pi} C_F \left(\frac{1}{\epsilon_{\text{UV}}} - \frac{1}{\epsilon_{\text{IR}}} + 2 \ln \frac{\mu_{\text{UV}}}{\mu_{\text{IR}}} \right) \Bigg[(-2y \ln y - 2\bar{y} \ln \bar{y}) \langle E_1 \rangle^{(0)} \\ - 4\epsilon \left(\ln y + \frac{\bar{y} \ln \bar{y}}{y} \right) \langle \mathcal{O}_1 \rangle^{(0)} \Bigg]. \end{aligned} \tag{99}$$

The renormalisation prescription tells us to subtract the UV-pole and the UV-finite part

of $\langle E_1\rangle$. So we obtain after renormalisation:

$$\langle E_1^{\text{ren.}}\rangle^{(1),(c)}_{\text{emitted}} = \frac{\alpha_s}{4\pi}C_F\Bigg[\left(-\frac{1}{\epsilon_{\text{IR}}}+2\ln\frac{\mu_{\text{UV}}}{\mu_{\text{IR}}}\right)(-2y\ln y-2\bar{y}\ln\bar{y})\,\langle E_1\rangle^{(0)} + 4\left(\ln y+\frac{\bar{y}\ln\bar{y}}{y}\right)\langle\mathcal{O}_1\rangle^{(0)}\Bigg]. \tag{100}$$

Note that the evanescent operator E_1 leads to a finite term $4(\ln y+\frac{\bar{y}\ln\bar{y}}{y})\langle\mathcal{O}_1\rangle^{(0)}$, which we would have missed if we had just dropped the evanescent operators.

5.2.4 Wave function of the recoiled pion

In the next step we consider the NLO contribution of the recoiled pion wave function. As in the case of the emitted pion the diagrams fig. 7(a),(b) do not lead to a mixing between the operators. Therefore we get:

$$\langle\mathcal{O}_1^{\text{ren.}}+\mathcal{O}_2^{\text{ren.}}\rangle^{(1),(a),(b)}_{\text{recoiled}} = \frac{\alpha_s}{4\pi}C_F\frac{2\ln\bar{x}+4x}{x}\Bigg[\left(-\frac{1}{\epsilon_{\text{IR}}}+2\ln\frac{\mu_{\text{UV}}}{\mu_{\text{IR}}}\right)\langle\mathcal{O}_1\rangle^{(0)} - \left(\frac{1}{\epsilon_{\text{IR}}}+2\ln\mu_{\text{IR}}\right)\langle\mathcal{O}_2\rangle^{(0)}\Bigg]. \tag{101}$$

Other than in the case of the emitted pion the operators $\mathcal{O}_1$ and $\mathcal{O}_2$ mix the spinors of the recoiled pion and the B-meson. Therefore we have to work in the operator basis of $\mathcal{O}_0$ and the evanescent operators and define our renormalisation scheme such that the finite parts of the matrix elements of the evanescent operators vanish. The diagram fig. 7(c) contributes to the matrix element of the renormalised operator $\mathcal{O}_0^{\text{ren.}}$:

$$\langle\mathcal{O}_0^{\text{ren.}}\rangle^{(1),(c)}_{\text{recoiled}} = 2\frac{\alpha_s}{4\pi}C_F\left(\frac{1}{\epsilon_{\text{IR}}}-2\ln\frac{\mu_{\text{UV}}}{\mu_{\text{IR}}}\right)\frac{\bar{x}\ln\bar{x}}{x}\langle\mathcal{O}_0\rangle^{(0)}. \tag{102}$$

In the case of the evanescent operators we keep the IR-pole:

$$\langle E_1^{\text{ren.}}\rangle^{(1),(c)}_{\text{recoiled}} = \frac{1}{2}\frac{\alpha_s}{4\pi}C_F\left(\frac{1}{\epsilon_{\text{IR}}}+2\ln\mu_{\text{IR}}\right)\frac{\bar{x}\ln\bar{x}}{x}\langle E_4\rangle^{(0)} \tag{103}$$

$$\langle E_2^{\text{ren.}}\rangle^{(1),(c)}_{\text{recoiled}} = \frac{1}{4}\frac{\alpha_s}{4\pi}C_F\left(\frac{1}{\epsilon_{\text{IR}}}+2\ln\mu_{\text{IR}}\right)\frac{\bar{x}\ln\bar{x}}{x}\langle E_3\rangle^{(0)} \tag{104}$$

At the end of the day we obtain a contribution from diagram fig. 7(c):

$$\langle\mathcal{O}_0^{\text{ren.}}+E_1^{\text{ren.}}+E_2^{\text{ren.}}\rangle^{(1),(c)}_{\text{recoiled}} = \frac{1}{2}\frac{\alpha_s}{4\pi}C_F\frac{\bar{x}\ln\bar{x}}{x}\Bigg[\left(\frac{1}{\epsilon_{\text{IR}}}-2\ln\frac{\mu_{\text{UV}}}{\mu_{\text{IR}}}\right)\langle\frac{1}{\bar{x}l^-}\gamma^\mu\gamma^\lambda\gamma^\tau\tilde{\otimes}\gamma_\tau\gamma_\lambda\gamma^\nu\otimes\left(\frac{2\not{p}g_{\mu\nu}}{\bar{y}}-\frac{\not{p}\gamma_\mu\gamma_\nu}{y\bar{y}}\right)\rangle^{(0)} + 8\langle\mathcal{O}_1\rangle^{(0)}\Bigg]. \tag{105}$$

The very complicated but also very explicit form, in which the above equation was given, is rather convenient, because the QCD amplitude $\mathcal{A}^{(2)}_{\text{spect.}}$ (see (78)-(80)) comes with the same Dirac structure and cancels the IR-pole of (105).

5.2.5 Wave function of the B-meson

The α_s corrections of the wave function of the B-meson are given by the second row of fig. 7. For the diagrams (d), (e) and (f) respectively they read:

$$\begin{aligned}
&\phi_{B\alpha\beta}^{(\mathrm{d}),(1)}(l'^-) = \qquad (106)\\
&\quad 8\pi^2 i\alpha_s N_c C_F \int \frac{d^dk}{(2\pi)^d} \frac{\delta(l'^- - l^- - k^-) - \delta(l'^- - l^-)}{k^2 k^-} \left[\bar{q}(l)\gamma^- \frac{1}{\not{k}+\not{l}}\right]_\beta b_\alpha(p+q-l)\\
&\phi_{B\alpha\beta}^{(\mathrm{e}),(1)}(l'^-) =\\
&\quad 8\pi^2 i\alpha_s N_c C_F \int \frac{d^dk}{(2\pi)^d} \frac{\delta(l'^- - l^- - k^-) - \delta(l'^- - l^-)}{k^2 k^-} \times\\
&\quad \bar{q}_\beta(l) \left[\frac{1}{\not{k}-\not{p}-\not{q}+\not{l}+m_b}\gamma^- b(p+q-l)\right]_\alpha\\
&\phi_{B\alpha\beta}^{(\mathrm{f}),(1)}(l'^-) =\\
&\quad 8\pi^2 i\alpha_s N_c C_F \int \frac{d^dk}{(2\pi)^d} \frac{\delta(l'^- - l^- - k^-)}{k^2} \times\\
&\quad \left[\bar{q}(l)\gamma^\mu \frac{1}{\not{k}+\not{l}}\right]_\beta \left[\frac{1}{\not{p}+\not{q}-\not{l}-\not{k}-m_b}\gamma_\mu b(p+q-l)\right]_\alpha
\end{aligned}$$

In the case of the B-meson only the diagrams in fig. 7(d),(e) give rise to UV-poles. Those diagrams however do not lead to a mixing of $\mathcal{O}_0$ and the evanescent operators and we do not have to deal with evanescent operators.

First let us have a look at the convolution integral which belongs to the diagram in fig. 7(f):

$$\begin{aligned}
&\langle \mathcal{O}_1 + \mathcal{O}_2\rangle_B^{(1),(\mathrm{f})} = \qquad (107)\\
&\quad (4\pi)^2 i\alpha_s^2 N_c C_F^2 \frac{1}{\bar{x}} \int \frac{d^dk}{(2\pi)^d} \frac{1}{2(k+l)\cdot p\, k^2} \times\\
&\quad \bar{q}_c\gamma^\tau \frac{\not{k}+\not{l}}{(k+l)^2}\gamma^\mu q_r' \bar{q}_r\gamma^\nu(1-\gamma_5)\frac{\not{p}+\not{q}-\not{l}-\not{k}+m_b}{k^2-2k\cdot(p+q-l)}\gamma_\tau b\bar{q}_e\left(\frac{2\not{p}}{\bar{y}}g_{\mu\nu} - \frac{\not{p}}{y\bar{y}}\gamma_\mu\gamma_\nu\right)(1-\gamma_5)q_e',
\end{aligned}$$

where q_c, $q_r^{(\prime)}$ and $q_e^{(\prime)}$ are the spinors carrying the flavour quantum numbers of the light constituent quark of the B-meson, the recoiled pion and the emitted pion respectively. In leading power (107) is identical to the contribution of the two diagrams shown in fig. 8, which is given by:

$$\begin{aligned}
&-(4\pi)^2 i\alpha_s^2 N_c C_F^2 \int \frac{d^dk}{(2\pi)^d} \frac{1}{k^2(k+l-\bar{x}p)^2}\\
&\quad \times \bar{q}_c\gamma^\tau \frac{\not{k}+\not{l}}{(k+l)^2}\gamma^\mu q_r'\bar{q}_r\gamma^\nu(1-\gamma_5)\frac{\not{p}+\not{q}-\not{l}-\not{k}+m_b}{k^2-2k\cdot(p+q-l)}\gamma_\tau b\\
&\quad \bar{q}_e\left(\gamma_\mu\frac{y\not{q}+\bar{x}\not{p}-\not{k}-\not{l}}{(yq+\bar{x}p-k-l)^2}\gamma_\nu - \gamma_\nu\frac{\bar{y}\not{q}+\bar{x}\not{p}-\not{k}-\not{l}}{(\bar{y}q+\bar{x}p-k-l)^2}\gamma_\mu\right)(1-\gamma_5)q_e'. \qquad (108)
\end{aligned}$$

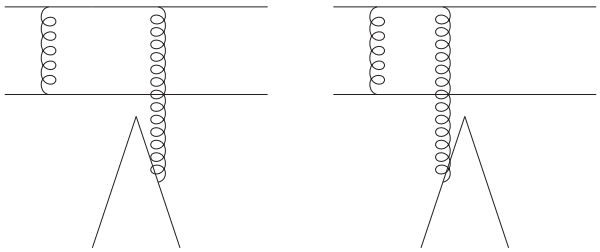

Figure 8: Two diagrams which correspond in leading power to the contribution of the B-meson wavefunction (107).

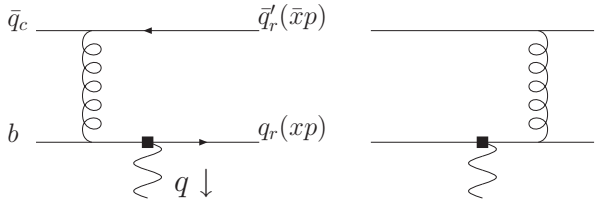

Figure 9: α_s contributions to the form factor

In (108) the leading power comes from the region where k is soft. In this region of space the integrand gets the form of the integrand in (107), so both contributions cancel. As we did not include the diagrams of fig. 8 in the last section we can skip the contribution of (107) here.

The remaining contributions are the diagrams in fig. 7(d) and (e). Together they read:

$$\begin{aligned}\langle \mathcal{O}_1 + \mathcal{O}_2 \rangle_B^{(1),(\mathrm{d}),(\mathrm{e})} = \\ \alpha_s^2 N_c C_F^2 \frac{1}{\xi\bar{x}} \bar{q}_c \gamma^\mu q'_r \bar{q}_r \gamma^\nu (1-\gamma_5) b \bar{q}_e \left(\frac{2\not{p}}{\bar{y}} g_{\mu\nu} - \frac{\not{p}}{y\bar{y}} \gamma_\mu \gamma_\nu \right) q'_e \times \\ \left(\left(\frac{1}{\epsilon_{\mathrm{UV}}} + 2\ln\frac{\mu_{\mathrm{UV}}}{m_b} \right)(4 + 2\ln\xi) - 2\left(\frac{1}{\epsilon_{\mathrm{IR}}} + 2\ln\frac{\mu_{\mathrm{IR}}}{m_b} \right) + 4 - \frac{2\pi^2}{3} - 2\ln^2\xi \right).\end{aligned} \tag{109}$$

5.2.6 Form factor contribution

Finally we have to calculate the contribution of (81). It is given by

$$\begin{aligned}\mathcal{A}_{\text{formfact.}} \equiv \phi_\pi^{(0)} \otimes \phi_\pi^{(0)} \otimes \phi_B^{(0)} \otimes T^{(1)}_{\text{formfact.}} \otimes T^{\mathrm{I}(1)} \equiv \\ \frac{C_F \alpha_s}{4\pi} f^{(1),\nu}\, \bar{q}_e(yq)\gamma_\nu(1-\gamma_5) q'_e(\bar{y}q)\, T^{(1)}(y).\end{aligned} \tag{110}$$

The form factor $f^{(1),\nu}$ is the α_s correction of the matrix element

$$\langle \bar{q}'_r(\bar{x}p) q_r(xp) | \bar{q}_r \gamma^\nu (1-\gamma_5) b | b(p+q-l)\bar{q}_c(l) \rangle, \tag{111}$$

where $T^{(1)}(y)$ is given by [12]:

$$T^{(1)}(y) = -6\left(\frac{1}{\epsilon}+\ln\frac{\mu^2}{m_b^2}\right)-18+3\left(\frac{1-2y}{\bar{y}}\ln y-i\pi\right)+ \left[2\mathrm{Li}_2(y)-\ln^2 y+\frac{2\ln y}{\bar{y}}-(3+2i\pi)\ln y-(y\leftrightarrow\bar{y})\right]. \tag{112}$$

We get $f^{(1),\nu}$ by evaluating the diagrams in fig. 9 and obtain finally:

$$\mathcal{A}_{\text{formfact.}} = \alpha_s^2 N_c C_F^2 \frac{1}{\bar{x}\xi}\bar{q}_c\gamma^\mu q_r'\bar{q}_r\left(\gamma_\mu\frac{\not{l}}{\xi}\gamma^\nu(1-\gamma_5)-\gamma^\nu(1-\gamma_5)\frac{x\not{p}+\not{q}+1}{\bar{x}}\gamma_\mu\right)b \bar{q}_e\gamma_\nu(1-\gamma_5)q_e' T^{(1)}(y). \tag{113}$$

6 NLO results

6.1 Analytical results for T_1^{II} and T_2^{II}

After the analysis of the last chapter we finally obtain the $\mathcal{O}(\alpha_s^2)$ results for the hard spectator scattering kernels $T_{1,2}^{\mathrm{II}}$ which are defined by (32). Those expressions appear in convolution integrals with wave functions, where x, y and ξ are the integration variables as defined in (32). The ultraviolet divergences are renormalised in the $\overline{\mathrm{MS}}$-scheme. The infrared divergences drop out after subtracting the wave function contributions from the amplitude. The infrared finiteness together with the finiteness of the convolution integrals ensures that the framework of QCD-factorization works at this order in α_s.

The explicit $\mathcal{O}(\alpha_s^2)$ contributions for $T_{1,2}^{\mathrm{II}}$ read (see next page):

$$
\begin{aligned}
\mathrm{Re}T_1^{\mathrm{II}(2)} \;=\; & -\frac{\alpha_s^2 C_F}{4N_c^2 m_B^2 \xi}\times \qquad (114)\\
& \Bigg[C_N\Bigg(-\frac{16\ln\xi}{3\bar{x}\bar{y}}-\frac{16\ln\bar{x}}{3\bar{x}\bar{y}}+\frac{40\ln\frac{\mu}{m_b}}{3\bar{x}\bar{y}}+\frac{80}{9\bar{x}\bar{y}}\Bigg)\\
& +C_F\Bigg(\left(\frac{4\ln\xi}{\bar{x}\bar{y}}+\frac{4\ln\bar{x}}{\bar{x}\bar{y}}+\frac{4\ln\bar{y}}{\bar{x}\bar{y}}+\frac{30}{\bar{x}\bar{y}}\right)\ln\frac{\mu}{m_b}\\
& \quad -\frac{\ln^2\xi}{\bar{x}\bar{y}}+\ln\xi\left(-\frac{2\ln x}{\bar{x}^2\bar{y}}-\frac{2\ln\bar{x}}{\bar{x}\bar{y}}-\frac{5}{\bar{x}\bar{y}}\right)\\
& \quad +\left(-\frac{2\bar{x}^2}{(y-\bar{x})^3}-\frac{4\bar{x}}{(y-\bar{x})^2}-\frac{2}{y-\bar{x}}-\frac{2x}{(y-x)\bar{x}}-\frac{2}{y\bar{x}^2}+\frac{2(5x-2)}{\bar{y}\bar{x}^2}\right)\mathrm{Li}_2 x\\
& \quad +\left(-\frac{2\bar{x}^2}{(y-\bar{x})^3}-\frac{4\bar{x}}{(y-\bar{x})^2}-\frac{2}{y-\bar{x}}+\frac{2x}{(y-x)\bar{x}}-\frac{4}{\bar{x}}+\frac{2}{y\bar{x}^2}+\frac{4}{\bar{y}\bar{x}^2}\right)\mathrm{Li}_2 y\\
& \quad +\left(\frac{2(x-2)}{\bar{x}^2\bar{y}}+\frac{2}{\bar{x}}\right)\mathrm{Li}_2(xy)\\
& \quad +\left(-\frac{2\bar{x}^2}{(y-\bar{x})^3}-\frac{4\bar{x}}{(y-\bar{x})^2}-\frac{2}{y-\bar{x}}\right)\mathrm{Li}_2\left(-\frac{xy}{\bar{x}}\right)\\
& \quad +\left(\frac{2x}{(y-x)\bar{x}}+\frac{2}{\bar{x}\bar{y}}\right)\mathrm{Li}_2\left(-\frac{y\bar{x}}{\bar{y}}\right)+\left(-\frac{2}{\bar{x}}+\frac{2}{\bar{x}^2\bar{y}}+\frac{2}{\bar{x}^2 y}\right)\mathrm{Li}_2(x\bar{y})\\
& \quad +\left(-\frac{2x}{(y-x)\bar{x}}-\frac{2}{\bar{x}\bar{y}}\right)\mathrm{Li}_2\left(-\frac{x\bar{y}}{\bar{x}}\right)\\
& \quad +\left(\frac{2\bar{x}^2}{(y-\bar{x})^3}+\frac{4\bar{x}}{(y-\bar{x})^2}+\frac{2}{y-\bar{x}}\right)\mathrm{Li}_2\left(-\frac{\bar{x}\bar{y}}{y}\right)\\
& \quad +\left(-\frac{2}{\bar{y}\bar{x}}-\frac{2}{\bar{x}}\right)\ln x\ln y+\frac{2(3x-2)\ln x\ln\bar{x}}{\bar{x}^2\bar{y}}+\left(\frac{2}{\bar{x}}+\frac{2}{\bar{y}\bar{x}^2}\right)\ln x\ln\bar{y}\\
& \quad +\left(-\frac{2\bar{x}^2}{(y-\bar{x})^3}-\frac{4\bar{x}}{(y-\bar{x})^2}-\frac{2}{y-\bar{x}}-\frac{2}{\bar{x}}+\frac{2}{y\bar{x}^2}+\frac{2x}{\bar{y}\bar{x}^2}\right)\ln y\ln\bar{y}\\
& \quad -\frac{2\ln\bar{x}\ln\bar{y}}{\bar{x}\bar{y}}+\frac{\ln^2 x}{\bar{x}\bar{y}}+\frac{\ln^2 y}{\bar{x}\bar{y}}-\frac{\ln^2\bar{x}}{\bar{x}\bar{y}}-\frac{2\ln^2\bar{y}}{\bar{x}\bar{y}}\\
& \quad +\left(-\frac{4-3x}{\bar{x}^2\bar{y}}-\frac{3}{\bar{x}}\right)\ln x+\left(\frac{2(3x-2)}{\bar{x}^2\bar{y}}+\frac{2\bar{x}}{(y-\bar{x})^2}+\frac{3}{y-\bar{x}}+\frac{3}{\bar{x}}\right)\ln y\\
& \quad +\left(\frac{-9x-1}{x\bar{x}\bar{y}}+\frac{2\bar{x}}{(y-\bar{x})^2}+\frac{3}{y-\bar{x}}-\frac{1-3x}{x^2 y\bar{x}}\right)\ln\bar{x}\\
& \quad +\left(-\frac{1}{\bar{x}\bar{y}}-\frac{4}{\bar{x}^2 y}\right)\ln\bar{y}+\left(\frac{4}{x\bar{x}\bar{y}}+\frac{4}{x\bar{x}^2 y}\right)\ln(1-xy)\\
& \quad +\left(-\frac{3x-1}{x^2 y\bar{x}}+\frac{-3x^2-2x-1}{x^2(y-\bar{x})}-\frac{3}{\bar{x}}-\frac{2}{\bar{x}^2\bar{y}}+\frac{2\,(x^2-1)}{x(y-\bar{x})^2}\right)\ln(1-x\bar{y})\\
& \quad +\frac{\pi^2\bar{x}^2}{3(y-\bar{x})^3}+\frac{2\pi^2\bar{x}}{3(y-\bar{x})^2}+\frac{\pi^2}{3(y-\bar{x})}+\frac{\pi^2}{3\bar{x}}-\frac{2\,(2\pi^2 x+63x-63)}{3\bar{y}\bar{x}^2}\Bigg)
\end{aligned}
$$

$$
\begin{aligned}
&-\frac{1}{2}C_G\Bigg(\frac{80\ln\frac{\mu}{m_b}}{3\bar{x}\bar{y}}+\left(-\frac{2\ln x}{\bar{x}^2\bar{y}}-\frac{22}{3\bar{x}\bar{y}}\right)\ln\xi\\
&\quad+\left(-\frac{2x}{(y-x)\bar{x}}+\frac{2\bar{x}}{(y-\bar{x})^2}+\frac{4}{y-\bar{x}}+\frac{2(5x-2)}{\bar{x}^2\bar{y}}-\frac{2}{y\bar{x}^2}\right)\mathrm{Li}_2 x\\
&\quad+\left(-\frac{2(x-3)}{\bar{x}^2\bar{y}}+\frac{2\bar{x}}{(y-\bar{x})^2}+\frac{4}{y-\bar{x}}+\frac{2x}{(y-x)\bar{x}}-\frac{4}{\bar{x}}+\frac{2}{y\bar{x}^2}\right)\mathrm{Li}_2 y\\
&\quad+\left(\frac{2(x-2)}{\bar{x}^2\bar{y}}+\frac{2}{\bar{x}}\right)\mathrm{Li}_2(xy)+\left(\frac{2\bar{x}}{(y-\bar{x})^2}+\frac{4}{y-\bar{x}}+\frac{2}{\bar{x}}\right)\mathrm{Li}_2\left(-\frac{xy}{\bar{x}}\right)\\
&\quad+\left(\frac{2x}{(y-x)\bar{x}}+\frac{2}{\bar{x}}\right)\mathrm{Li}_2\left(-\frac{y\bar{x}}{\bar{y}}\right)+\left(-\frac{2}{\bar{x}}+\frac{2}{\bar{x}^2\bar{y}}+\frac{2}{\bar{x}^2 y}\right)\mathrm{Li}_2(x\bar{y})\\
&\quad+\left(-\frac{2x}{(y-x)\bar{x}}-\frac{2}{\bar{x}}\right)\mathrm{Li}_2\left(-\frac{x\bar{y}}{\bar{x}}\right)\\
&\quad+\left(-\frac{2\bar{x}}{(y-\bar{x})^2}-\frac{4}{y-\bar{x}}-\frac{2}{\bar{x}}\right)\mathrm{Li}_2\left(-\frac{\bar{x}\bar{y}}{y}\right)\\
&\quad-\frac{2\ln x\ln y}{\bar{x}\bar{y}}+\frac{2(3x-2)\ln x\ln\bar{x}}{\bar{x}^2\bar{y}}+\left(\frac{2}{\bar{x}\bar{y}}-\frac{2}{\bar{x}}\right)\ln y\ln\bar{x}\\
&\quad+\frac{2\ln x\ln\bar{y}}{\bar{x}^2\bar{y}}+\left(\frac{2\bar{x}}{(y-\bar{x})^2}+\frac{4}{y-\bar{x}}-\frac{2}{\bar{x}}+\frac{2}{y\bar{x}^2}+\frac{2}{\bar{y}\bar{x}^2}\right)\ln y\ln\bar{y}\\
&\quad+\frac{2\ln\bar{x}\ln\bar{y}}{\bar{x}}+\frac{\ln^2 x}{\bar{x}\bar{y}}+\frac{\ln^2 y}{\bar{x}}-\frac{\ln^2\bar{x}}{\bar{x}\bar{y}}-\frac{\ln^2\bar{y}}{\bar{x}}\\
&\quad-\frac{(4-3x)\ln x}{\bar{x}^2\bar{y}}+\left(-\frac{3-5x}{\bar{x}^2\bar{y}}-\frac{2}{y-\bar{x}}\right)\ln y\\
&\quad+\left(\frac{2}{x\bar{x}\bar{y}}+\frac{2}{x\bar{x}^2 y}\right)\ln(1-xy)+\left(\frac{2}{xy\bar{x}}-\frac{31}{3\bar{x}\bar{y}}-\frac{2}{y-\bar{x}}\right)\ln\bar{x}\\
&\quad-\frac{2\ln\bar{y}}{y\bar{x}^2}+\left(\frac{2(x+1)}{x(y-\bar{x})}-\frac{2}{xy\bar{x}}-\frac{2}{\bar{x}^2\bar{y}}\right)\ln(1-x\bar{y})\\
&\quad-\frac{2\left(3\pi^2x+166x+3\pi^2-166\right)}{9\bar{x}^2\bar{y}}-\frac{\pi^2\bar{x}}{3(y-\bar{x})^2}-\frac{2\pi^2}{3(y-\bar{x})}+\frac{\pi^2}{3\bar{x}}\Bigg)\Bigg]
\end{aligned}
$$

$$
\begin{aligned}
\mathrm{Im}T_1^{\mathrm{II}(2)} \;=\; &-\frac{2\pi\alpha_s^2 C_F}{4N_c^2 m_B^2\xi}\times \qquad (115)\\
&\Bigg[C_F\Bigg(-\frac{x\ln x}{\bar{x}^2\bar{y}}+\left(\frac{\bar{x}^2}{(y-\bar{x})^3}+\frac{2\bar{x}}{(y-\bar{x})^2}+\frac{1}{y-\bar{x}}+\frac{1}{\bar{y}\bar{x}}\right)\ln y\\
&\quad+\left(-\frac{\bar{x}^2}{(y-\bar{x})^3}-\frac{2\bar{x}}{(y-\bar{x})^2}-\frac{1}{y-\bar{x}}-\frac{x}{(y-x)\bar{x}}-\frac{1}{\bar{y}\bar{x}}\right)\ln\bar{x}\\
&\quad+\left(\frac{x}{(y-x)\bar{x}}+\frac{1}{\bar{x}\bar{y}}\right)\ln\bar{y}-\frac{\bar{x}}{(y-\bar{x})^2}-\frac{3}{2(y-\bar{x})}+\frac{2}{\bar{y}\bar{x}}\Bigg)
\end{aligned}
$$

$$
\begin{aligned}
&-\frac{1}{2}C_G\bigg(-\frac{x\ln x}{\bar{x}^2\bar{y}}+\bigg(-\frac{\bar{x}}{(y-\bar{x})^2}-\frac{2}{y-\bar{x}}\bigg)\ln y\\
&\qquad+\bigg(-\frac{x}{(y-x)\bar{x}}+\frac{\bar{x}}{(y-\bar{x})^2}+\frac{2}{y-\bar{x}}-\frac{1}{\bar{x}\bar{y}}\bigg)\ln\bar{x}\\
&\qquad+\frac{x\ln\bar{y}}{(y-x)\bar{x}}+\frac{3}{2\bar{x}\bar{y}}+\frac{1}{y-\bar{x}}\bigg)\bigg]
\end{aligned}
$$

$$
\begin{aligned}
\mathrm{Re}T_2^{\mathrm{II}} \;=\; & -\frac{\alpha_s^2 C_F C_N}{4N_c^2 m_B^2\xi}\times \qquad (116)\\
&\bigg[\frac{12\ln\frac{\mu}{m_b}}{\bar{x}\bar{y}}+\bigg(-\frac{2\bar{x}^2}{(y-\bar{x})^3}-\frac{4\bar{x}}{(y-\bar{x})^2}-\frac{2}{y-\bar{x}}-\frac{2x}{(y-x)\bar{x}}-\frac{2}{\bar{y}\bar{x}}\bigg)\mathrm{Li}_2 x\\
&+\frac{2x\mathrm{Li}_2 y}{(y-x)\bar{x}}+\bigg(-\frac{2\bar{x}^2}{(y-\bar{x})^3}-\frac{4\bar{x}}{(y-\bar{x})^2}-\frac{2}{y-\bar{x}}\bigg)\mathrm{Li}_2\left(-\frac{xy}{\bar{x}}\right)\\
&+\bigg(\frac{2x}{(y-x)\bar{x}}+\frac{2}{\bar{x}\bar{y}}\bigg)\mathrm{Li}_2\left(-\frac{y\bar{x}}{\bar{y}}\right)\\
&+\bigg(\frac{2\bar{x}^2}{(y-\bar{x})^3}+\frac{4\bar{x}}{(y-\bar{x})^2}+\frac{2}{y-\bar{x}}+\frac{2}{\bar{y}\bar{x}}\bigg)\mathrm{Li}_2\bar{y}\\
&+\bigg(-\frac{2x}{(y-x)\bar{x}}-\frac{2}{\bar{x}\bar{y}}\bigg)\mathrm{Li}_2\left(-\frac{x\bar{y}}{\bar{x}}\right)\\
&+\bigg(\frac{2\bar{x}^2}{(y-\bar{x})^3}+\frac{4\bar{x}}{(y-\bar{x})^2}+\frac{2}{y-\bar{x}}\bigg)\mathrm{Li}_2\left(-\frac{\bar{x}\bar{y}}{y}\right)\\
&-\frac{2\ln x\ln y}{\bar{x}\bar{y}}+\frac{2\ln x\ln\bar{y}}{\bar{x}\bar{y}}+\frac{\ln^2 y}{\bar{x}\bar{y}}-\frac{\ln^2\bar{y}}{\bar{x}\bar{y}}-\frac{(2-3x)\ln x}{\bar{x}^2\bar{y}}\\
&+\bigg(\frac{x-2}{\bar{x}^2\bar{y}^2}+\frac{2\bar{x}}{(y-\bar{x})^2}+\frac{3}{y-\bar{x}}+\frac{x}{\bar{x}^2\bar{y}}\bigg)\ln y\\
&+\bigg(\frac{2}{x\bar{x}\bar{y}}+\frac{2}{x\bar{x}^2 y}\bigg)\ln(1-xy)+\bigg(\frac{2\bar{x}}{(y-\bar{x})^2}+\frac{3}{y-\bar{x}}\bigg)\ln\bar{x}\\
&+\bigg(\frac{-3x^2-2x-1}{x^2(y-\bar{x})}-\frac{1}{x^2\bar{x}^2\bar{y}}+\frac{2\,(x^2-1)}{x(y-\bar{x})^2}+\frac{1}{x\bar{x}^2\bar{y}^2}\bigg)\ln(1-x\bar{y})\\
&+\bigg(-\frac{3}{\bar{x}\bar{y}}-\frac{2}{\bar{x}^2 y}\bigg)\ln\bar{y}+\frac{16}{\bar{x}\bar{y}}\bigg]
\end{aligned}
$$

$$
\begin{aligned}
\mathrm{Im}T_2^{\mathrm{II}} &= -\frac{2\pi\alpha_s^2 C_F C_N}{4N_c^2 m_B^2 \xi}\times \qquad (117)\\
&\left[\left(\frac{\bar{x}^2}{(y-\bar{x})^3}+\frac{2\bar{x}}{(y-\bar{x})^2}+\frac{1}{y-\bar{x}}+\frac{1}{\bar{y}\bar{x}}\right)\ln y\right.\\
&+\left(-\frac{\bar{x}^2}{(y-\bar{x})^3}-\frac{2\bar{x}}{(y-\bar{x})^2}-\frac{1}{y-\bar{x}}-\frac{x}{(y-x)\bar{x}}-\frac{1}{\bar{y}\bar{x}}\right)\ln\bar{x}\\
&\left.+\frac{x\ln\bar{y}}{(y-x)\bar{x}}-\frac{\bar{x}}{(y-\bar{x})^2}-\frac{3}{2(y-\bar{x})}+\frac{3}{2\bar{y}\bar{x}}\right]
\end{aligned}
$$

The α_s^2 corrections of the hard spectator interactions have already been calculated in [3, 4]. However both of these calculations have been performed in the framework of SCET, while my result is a pure QCD calculation. In order to compare (114)-(117) to [3, 4] we have to take into account the definition of λ_B. The SCET calculation naturally uses the λ_B defined by the HQET field for the b-meson, while I define λ_B by QCD-fields. Those two definitons differ at $\mathcal{O}(\alpha_s)$, which has been discussed in [25]. The difference in the logarithmic moments of the B-meson wave function does not play a role, because these moments occur first at NLO. Using the results of [25] it is easy to figure out with the help of a computer algebra system, that (114)-(117) reproduce the results of [3, 4].

6.2 Convolution integrals and factorizability

By looking at the hard scattering kernels of (114)-(117) it is not obvious that there remain no singularities in the convolution integrals over wave functions (32). It is however possible to perform the integration analytically, which proves the factorizabilty.

Regarding the B-meson wave function we will obtain the result in terms of the quantities λ_B and λ_n, which are defined in (16) and (17). The π-meson wave function is given in terms of Gegenbauer polynomials:

$$
\phi_\pi(x) = 6x\bar{x}\left[1+\sum_{n=1}^{\infty} a_n^\pi C_n^{(3/2)}(2x-1)\right]. \qquad (118)
$$

Due to the symmetry properties of the pion the first non vanishing moment is a_2^π. We

neglect a_n^π for $n > 2$ and using (32) we get for the NLO of $A_{\rm spect}$:

$$
\begin{aligned}
A^{(2)}_{\text{spect. 1}} = \alpha_s^2 \frac{i f_\pi^2 f_B}{4N_c^2} C_F \frac{m_B}{\lambda_B} \times \\
\Bigg[C_N \left(120 \ln \frac{\mu}{m_b} - 48\lambda_1 + 152 \right) \\
+ C_F \Bigg((162 + 36\lambda_1) \ln \frac{\mu}{m_b} - 9\lambda_2 + (-54 + 6\pi^2)\lambda_1 + \frac{1566}{5} - \frac{1008}{5}\zeta(3) + 27\pi^2 \\
+ i \left(-9\pi + \frac{18}{5}\pi^3 \right) \Bigg) \\
- \frac{1}{2} C_G \Bigg(240 \ln \frac{\mu}{m_b} + (-102 + 6\pi^2)\lambda_1 + \frac{2101}{5} - \frac{1008}{5}\zeta(3) + 18\pi^2 \\
+ i \left(9\pi + \frac{18}{5}\pi^3 \right) \Bigg) \\
+ a_2^\pi \Bigg\{ C_N \left(240 \ln \frac{\mu}{m_b} - 96\lambda_1 + 404 \right) \\
+ C_F \Bigg((174 + 72\lambda_1) \ln \frac{\mu}{m_b} - 18\lambda_2 + \left(-\frac{741}{2} + 42\pi^2 \right) \lambda_1 - \frac{14809}{35} \\
- \frac{45072}{35}\zeta(3) + 204\pi^2 + i \left(-338\pi + \frac{1362}{35}\pi^3 \right) \Bigg) \\
- \frac{1}{2} C_G \Bigg(480 \ln \frac{\mu}{m_b} + (-504 + 42\pi^2)\lambda_1 + \frac{22299}{35} - \frac{43992}{35}\zeta(3) + 161\pi^2 \\
+ i \left(-292\pi + \frac{1482}{35}\pi^3 \right) \Bigg) \Bigg\} \Bigg] \qquad (119)
\end{aligned}
$$

and

$$
\begin{aligned}
A^{(2)}_{\text{spect. 2}} = \alpha_s^2 \frac{i f_\pi^2 f_B}{4N_c^2} C_F C_N \frac{m_B}{\lambda_B} \times \\
\Bigg[108 \ln \frac{\mu}{m_b} + \frac{1467}{10} + \frac{252}{5}\zeta(3) - 6\pi^2 + i \left(54\pi - \frac{12}{5}\pi^3 \right) \\
+ a_2^\pi \left(216 \ln \frac{\mu}{m_b} + \frac{40281}{140} + \frac{29268}{35}\zeta(3) - 112\pi^2 + i \left(118\pi - \frac{108}{35}\pi^3 \right) \right) \Bigg]. \qquad (120)
\end{aligned}
$$

The finiteness of the above equations proves factorization of the hard spectator interactions at NLO.

Including the contributions of $A^{(2)}_{\text{spect. 1}}$ and $A^{(2)}_{\text{spect. 2}}$ the quantities $a_{1,\text{II}}$ and $a_{2,\text{II}}$ defined

CKM-parameters					
$V_{\rm ud}$ [26]	$V_{\rm cd}$	$V_{\rm cb}$ [26]	$\lvert V_{\rm ub}/V_{\rm cb}\rvert$ [26]		γ
0.974	-0.23	0.041	0.09±0.025		(70±20)deg
Parameters of the B-meson					
m_B	f_B [27]	$\frac{f_B}{f_+^{B\pi}\lambda_B}$ [28]	λ_1 [3]	λ_2 [3]	$\tau_{B^\pm}$	τ_{B^0}
5.28GeV	(210±19)MeV	1.56 ± 0.17	-3.2 ± 1	11 ± 4	1.67 ps	1.54 ps
Parameters of the π-meson					
$f_+^{B\pi}$ [29, 30, 31]		f_π	m_π	a_1^π	a_2^π [32, 33]
0.28 ± 0.05		131MeV	130MeV	0	0.3 ± 0.15
Quark and W-boson masses					
$m_b(m_b)$	$m_c(m_b)$	$m_t(m_t)$ [12]			M_W
4.2 GeV	(1.3±0.2) GeV	167 GeV			80.4 GeV
Coupling constants					
$\Lambda^{(5)}_{\overline{\rm MS}}$	G_F				
225 MeV	$1.16639 \times 10^{-5}\,{\rm GeV}^{-2}$				

Table 1: Input parameters, which were used in the numerical analysis. All parameters given without explicit citation can be found in [34]. Unless otherwise stated scale dependent quantities are given at $\mu = 1$GeV.

in (22) and (24) are

$$\begin{aligned} a_{1,\rm II} &= \frac{i}{f_\pi f_+^{B\pi} m_B^2}(C_2 A^{(1)}_{\text{spect. }1} + C_2 A^{(2)}_{\text{spect. }1} + C_1 A^{(2)}_{\text{spect. }2}) \\ a_{2,\rm II} &= \frac{i}{f_\pi f_+^{B\pi} m_B^2}(C_1 A^{(1)}_{\text{spect. }1} + C_1 A^{(2)}_{\text{spect. }1} + C_2 A^{(2)}_{\text{spect. }2}), \end{aligned} \tag{121}$$

where

$$A^{(1)}_{\text{spect. }1} = \frac{-iC_F\pi\alpha_s}{N_c^2}\frac{f_B f_\pi^2 m_B}{\lambda_B} 9(1+a_2^\pi)^2. \tag{122}$$

7 Numerical analysis

7.1 Input parameters

For my numerical analysis I use the parameters given in table 1. The decay constant f_B and the ratio $\frac{f_B}{f_+^{B\pi}\lambda_B}$ have been obtained by QCD sum rules in [27] and [28] respectively. The logarithmic moments λ_1 and λ_2 where calculated in [3] using model light-cone wave functions for the B-meson [35, 36, 37, 38]. For the form factor $f_+^{B\pi}$ I use the value from

[31], which has been obtained by QCD sum rules. This value is consistent with quenched and recent unquenched lattice calculations [29, 30]. The first Gegenbauer moment of the pion wave function is zero due to G-parity while the second moment has been obtained by lattice simulations [32, 33].

7.2 Amplitudes a_1 and a_2

The QCD amplitudes a_1 and a_2 are defined in [12]. Their hard scattering parts $a_{1,\mathrm{II}}$ and $a_{2,\mathrm{II}}$, i.e. the parts of a_1 and a_2, which contribute to $\mathcal{A}^{\mathrm{II}}$ (see (21)), are plotted in fig. 10 as functions of the renormalisation scale μ. The strong dependence on μ of the real part of LO is reduced at NLO. Taking the twist-3 contributions into account does not increase the μ-dependence too much. The imaginary part, which occurs first at NLO, is strongly dependent on the renormalisation scale. An appropriate choice for the scale of the hard scattering amplitude is the hard collinear scale

$$\mu_{\mathrm{hc}} = 1.5\mathrm{GeV} \tag{123}$$

In the following numerical calculations we will evaluate $a_{1,\mathrm{II}}$ and $a_{2,\mathrm{II}}$ at μ_{hc}. The vertex corrections $\mathcal{A}^{\mathrm{I}}$ will be evaluated at

$$\mu_b = 4.8\mathrm{GeV}. \tag{124}$$

Using the parameters of table 1 we obtain

$$\begin{aligned} a_1 =& 1.015 + [0.039 + 0.018i]_V + [-0.012]_{\mathrm{tw3}} + [-0.029]_{\mathrm{LO}} \\ &+ [-0.010 - 0.031i]_{\mathrm{NLO}} \\ a_2 =& 0.184 + [-0.171 - 0.080i]_V + [0.038]_{\mathrm{tw3}} + [0.096]_{\mathrm{LO}} \\ &+ [0.021 + 0.045i]_{\mathrm{NLO}}. \end{aligned} \tag{125}$$

These equations are given in a form similar to (61) and (62) in [3]. The first number gives the tree contribution, the vertex corrections are indicated by the label V, the twist-3 contributions are labelled by tw3. The hard scattering part is separated into LO and NLO. The hadronic input parameters I used are slightly different from [3] and in contrast to [3] I evaluated all quantities, which belong to the hard scattering amplitude, at the hard collinear scale μ_{hc}. This is why the values I get for a_1 and a_2 are different from [3].

The hard scattering amplitudes $a_{1,\mathrm{II}}$ and $a_{2,\mathrm{II}}$ together with their numerical errors read:

$$\begin{aligned} a_{1,\mathrm{II}} =& -0.051 \pm 0.011(\mathrm{param.})^{+0.026}_{-0.005}(\mathrm{scale}) \pm 0.012(\mathrm{tw3}) \\ &+ [-0.031 \pm 0.008(\mathrm{param.})^{+0.024}_{-0.031}(\mathrm{scale}) \pm 0.012(\mathrm{tw3})]i \\ a_{2,\mathrm{II}} =& 0.15 \pm 0.03(\mathrm{param.})^{+0.01}_{-0.04}(\mathrm{scale}) \pm 0.04(\mathrm{tw3}) \\ &+ [0.045 \pm 0.012(\mathrm{param.})^{+0.040}_{-0.033}(\mathrm{scale}) \pm 0.038(\mathrm{tw3})]i. \end{aligned} \tag{126}$$

The first error comes from the error of the input parameters in table 1. The scale uncertainty is obtained by varying μ_{hc} between 1GeV and 6GeV. The error labelled by tw3 gives

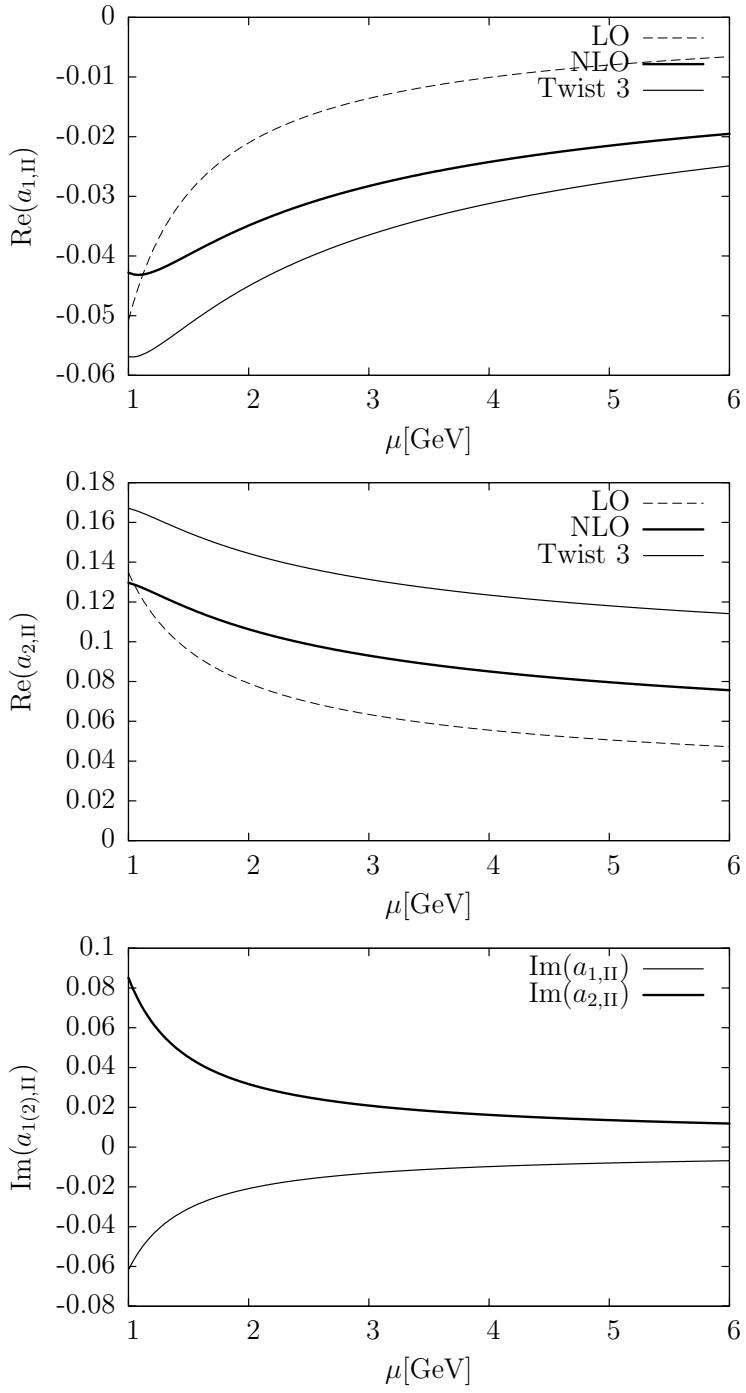

Figure 10: Contribution of the hard spectator corrections to a_1 and a_2 as a function of the renormalisation scale μ. The upper two figures show the real part, where the LO is given by the dashed line, while the sum of LO and NLO is shown by the thick solid line. The twist-3 corrections are included in the graph given by the thin solid line. The third figure shows the imaginary part, which occurs first at $\mathcal{O}(\alpha_s^2)$. So no distinction between LO and NLO is made.

the error of the twist-3 contribution. Within the scale uncertainty (126) is compatible with [3]. The result I obtained in QCD comes with formally large logarithms $\ln \Lambda_{\rm QCD}/m_b$. Without resummation these logarithms might spoil perturbation theory. However the error coming from the scale uncertainty in (126) as well as the relative size of the NLO contributions are small enough for perturbation theory to be valid.

7.3 Branching ratios

The dependence of the CP-averaged branching ratios on the hard collinear scale is shown in fig. 11. It is obvious that the NLO corrections reduce this dependence significantly.

From the parameter set table 1 we obtain the following CP-averaged branching ratios

$$\begin{aligned}
10^6 \mathrm{BR}(B^+ \to \pi^+\pi^0) &= 6.05^{+2.36}_{-1.98}(\mathrm{had.})^{+2.90}_{-2.33}(\mathrm{CKM})^{+0.18}_{-0.31}(\mathrm{scale}) \pm 0.27(\mathrm{sublead.}) \\
10^6 \mathrm{BR}(B^0 \to \pi^+\pi^-) &= 9.41^{+3.56}_{-2.99}(\mathrm{had.})^{+4.00}_{-3.46}(\mathrm{CKM})^{+1.07}_{-3.93}(\mathrm{scale})^{+1.13}_{-0.70}(\mathrm{sublead.}) \\
10^6 \mathrm{BR}(B^0 \to \pi^0\pi^0) &= 0.39^{+0.14}_{-0.12}(\mathrm{had.})^{+0.20}_{-0.17}(\mathrm{CKM})^{+0.17}_{-0.06}(\mathrm{scale})^{+0.20}_{-0.08}(\mathrm{sublead.}).
\end{aligned} \tag{127}$$

The origin of the errors are the uncertainties of the hadronic parameters and the CKM parameters, the scale dependence and the subleading power contributions, i.e. twist-3 and annihilation contributions. The error arising from the scale dependence was estimated by varying μ_b between 2GeV and 8GeV and $\mu_{\rm hc}$ between 1GeV and 6GeV. If we compare (127) to the experimental values [39]:

$$\begin{aligned}
10^6 \mathrm{BR}(B^+ \to \pi^+\pi^0) &= 5.5 \pm 0.6 \\
10^6 \mathrm{BR}(B^0 \to \pi^+\pi^-) &= 5.0 \pm 0.4 \\
10^6 \mathrm{BR}(B^0 \to \pi^0\pi^0) &= 1.45 \pm 0.29
\end{aligned} \tag{128}$$

we note that $\mathrm{BR}(B^+ \to \pi^+\pi^0)$ is in good agreement with the data. For $B^+ \to \pi^+\pi^0$ and $B^0 \to \pi^+\pi^-$ QCD-factorization is expected to work well, because at tree level Wilson coefficients occur in the so called colour allowed combination $C_1 + C_2/N_c \sim 1$, while $B^0 \to \pi^0\pi^0$ comes at tree level with $C_2 + C_1/N_c \sim 0.2$ such that subleading power corrections are expected to be more important. On the other hand there are big uncertainties in the parameters occurring in the combinations $|V_{ub}| f_+^{B\pi}$, $\frac{f_B}{f_+^{B\pi}\lambda_B}$ and a_2^π. In [40] and [3] these parameters were fitted by the experimental values (128) of $\mathrm{BR}(B^+ \to \pi^+\pi^0)$ and $\mathrm{BR}(B^0 \to \pi^+\pi^-)$. Setting

$$a_2^\pi(1\mathrm{GeV}) = 0.39 \tag{129}$$

leads to

$$\begin{aligned}
|V_{ub}| f_+^{B\pi} &\to 0.80 \left(|V_{ub}| f_+^{B\pi}\right)_{\rm default} \\
\frac{f_B}{f_+^{B\pi}\lambda_B} &\to 2.89 \left(\frac{f_B}{f_+^{B\pi}\lambda_B}\right)_{\rm default}.
\end{aligned} \tag{130}$$

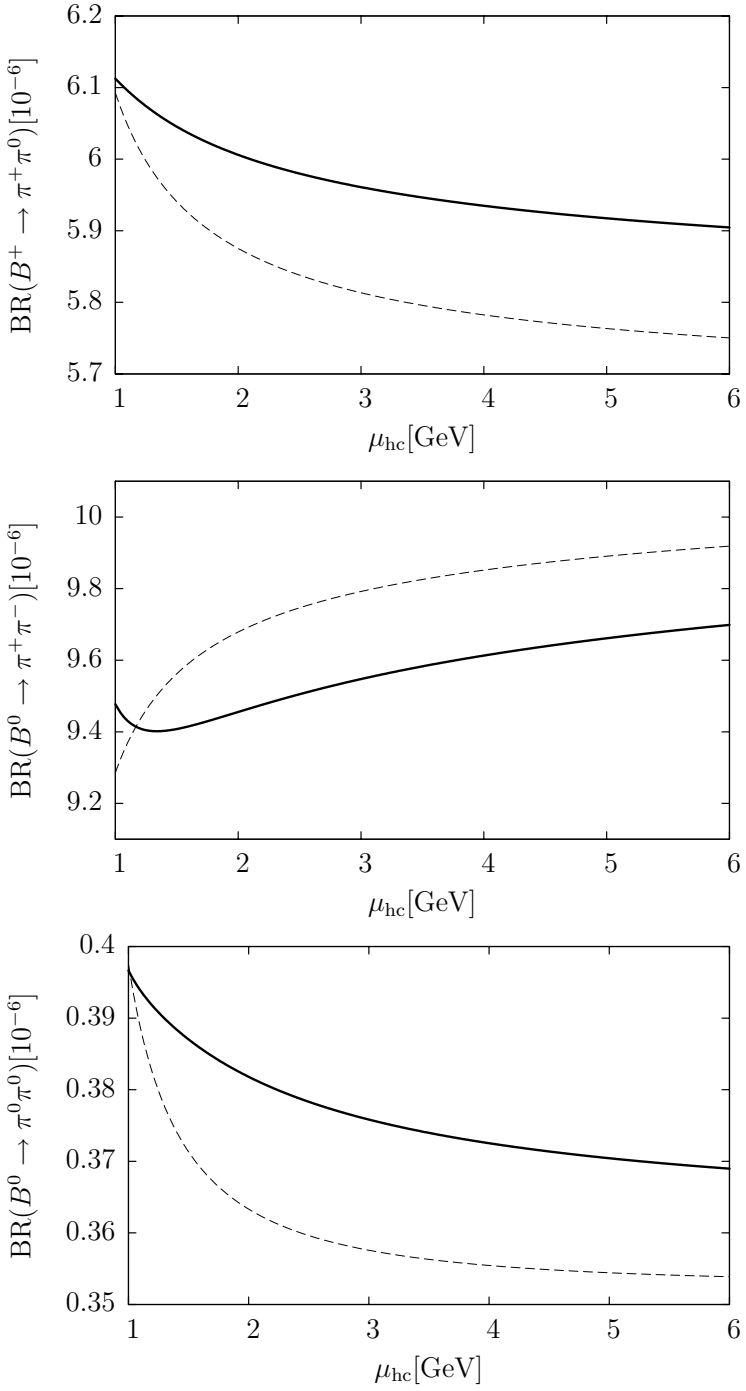

Figure 11: CP-averaged branching ratios as functions of the hard collinear scale $\mu_{\rm hc}$ in units of 10^{-6}. In the graph with the dashed line only the leading order of the hard spectator scattering is contained, while in the solid line hard spectator scattering is taken into account up to NLO.

This leads to the following branching ratios:

$$\begin{aligned} 10^6 \mathrm{BR}(B^+ \to \pi^+\pi^0) &= 5.5 \pm 0.2(\mathrm{param.})^{+0.5}_{-0.3}(\mathrm{scale}) \pm 0.6(\mathrm{sublead.}) \\ 10^6 \mathrm{BR}(B^0 \to \pi^+\pi^-) &= 5.0^{+0.8}_{-0.9}(\mathrm{param.})^{+0.9}_{-0.2}(\mathrm{scale})^{+0.9}_{-0.6}(\mathrm{sublead.}) \\ 10^6 \mathrm{BR}(B^0 \to \pi^0\pi^0) &= 0.77 \pm 0.3(\mathrm{param.})^{+0.2}_{-0.3}(\mathrm{scale})^{+0.3}_{-0.2}(\mathrm{sublead.}). \end{aligned} \tag{131}$$

The uncertainties of the quantities that occurred in (129) and (130) have not been considered in the estimation of the errors in (131). The $B^0 \to \pi^0\pi^0$ branching ratio obtained in (131) is compatible with the value obtained in [3]. Though it is too low, due to the theoretical and experimental errors it is compatible with (128).

8 Conclusions

QCD factorization has turned out to be an appropriate tool to calculate B decay modes from first principles, because it allows us to disentangle systematically the perturbative physics and the non-perturbative physics. The present calculation showed that the hard spectator scattering amplitude factorizes up to $\mathcal{O}(\alpha_s^2)$, i.e. all infrared divergences cancel and there are no remaining endpoint singularities. The former point is obvious after the explicit calculation of T^{II} and the latter point was shown by evaluating the convolution integral (1) analytically. The explicit expressions for the hard spectator scattering kernel (114)-(117) confirmed the result of [3, 4]. So they are also a confirmation that the leading power of the amplitudes can be obtained by performing the power expansion at the level of Feynman integrals rather than at the level of the QCD Lagrangian using an effective theory like SCET, which was done in [3, 4].

The main challenges in the evaluation of Feynman integrals were due to the fact that the Feynman integrals came with up to five external legs and three independent rations of scales. The calculation of the Feynman integrals was made possible with the help of tools like integration by parts identities and differential equation techniques: In section 4 it was shown how to get the expansion of Feynman integrals in powers of $\Lambda_{\mathrm{QCD}}/m_b$ by differential equations once the leading power is given.

Because next to the m_b-scale also the hard-collinear scale $\sqrt{\Lambda_{\mathrm{QCD}} m_b}$ enters the hard spectator scattering amplitude, large logarithms could spoil perturbation theory. However the numerical analysis showed a strong reduction of the scale uncertainty of T^{II}. It also confirmed the observation of [3], that the NLO of T^{II} is numerically important but small enough for perturbation theory to be valid.

Finally it is important to note that in the present calculation the contributions of penguin contractions and the effective penguin operators were not considered. Actually they play a dominant role in the branching ratios of $B \to K\pi$ and CP asymmetries of $B \to \pi\pi$ and should be taken into account in phenomenological applications. They have recently been published in [8]. Also the $\mathcal{O}(\alpha_s^2)$ corrections of T^{I} were not part of the present work. These contributions have been calculated in [9, 10].

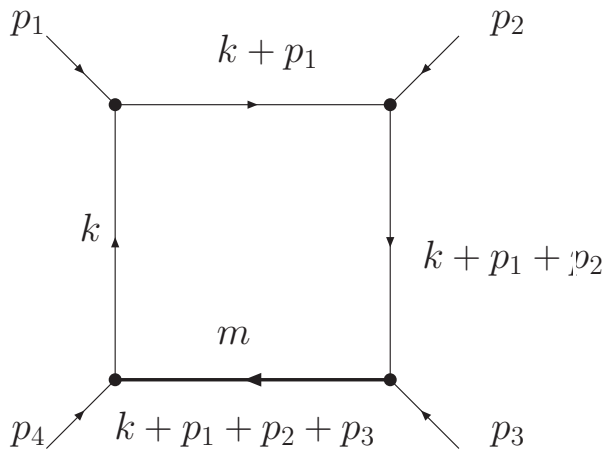

Figure 12: Basic one-loop four-point intergral. The massive line, which carries the mass m, is indicated by the thick line.

Acknowledgements

I would like to thank Gerhard Buchalla for proofreading the drafts and comments on the manuscript. I am grateful to Guido Bell, Matthäus Bartsch and Sebastian Jäger for many instructive and helpful discussions.

A Massive four-point integral

We consider the following massive four-point integral in $d = 4 - 2\epsilon$ dimensions (fig. 12):

$$I_4(p_1, p_2, p_3, p_4) = \mu^{2\epsilon} \int \frac{d^d k}{(2\pi)^d} \frac{1}{D_1 D_2 D_3 D_4} \tag{132}$$

where

$$\begin{aligned} D_1 &= k^2 + i\eta \\ D_2 &= (k + p_1)^2 + i\eta \\ D_3 &= (k + p_1 + p_2)^2 + i\eta \\ D_4 &= (k + p_1 + p_2 + p_3 + p_4)^2 - m^2 + i\eta \end{aligned} \tag{133}$$

Following [21] we introduce the external masses

$$p_i^2 = m_i^2 \quad (i = 1, 2, 3, 4) \tag{134}$$

and the Mandelstam variables

$$s = (p_1 + p_2)^2, \quad t = (p_2 + p_3)^2. \tag{135}$$

Furthermore we consider only the case, where

$$m_2^2 = 0 \quad \text{and} \quad m_4^2 = m^2. \tag{136}$$

The integral (132) can be evaluated using the method of [21]. This paper gives explicit expressions for massless one-loop box integrals. It is however possible to extend the single steps of this paper to our case.

So finally we obtain:

$$\begin{aligned}
I_4(p_1,p_2,p_3,p_4) \equiv I_4(s,t,m_1^2,m_3^2,m^2) &= \frac{i}{(4\pi)^2}\frac{\Gamma(1+\epsilon)(4\pi\mu^2)^\epsilon}{m^2(s-m_1^2)-st+m_1^2m_3^2} \\
\times\Bigg[&\frac{1}{\epsilon}\left(\ln(-s-i\eta)+\ln(m^2-t-i\eta)-\ln(m^2-m_3^2-i\eta)-\ln(-m_1^2-i\eta)\right) \\
&+\ln^2(m^2-m_3^2-i\eta)+\ln^2(-m_1^2-i\eta)-\ln^2(-s-i\eta)-\ln^2(m^2-t-i\eta) \\
&+\ln(m^2-i\eta)\left(\ln(-s-i\eta)+\ln(m^2-t-i\eta)-\ln(m^2-m_3^2-i\eta)-\ln(-m_1^2-i\eta)\right) \\
&+2\mathrm{Li}_2\left(1-\frac{m^2-t-i\eta}{-m_1^2-i\eta}\right)-2\mathrm{Li}_2\left(1-\frac{m^2-m_3^2-i\eta}{-s-i\eta}\right) \\
&+2\mathrm{Li}_2\left(1-(m_3^2-m^2+i\eta)f^m\right)+2\mathrm{Li}_2\left(1-(m_1^2+i\eta)f^m\right) \\
&-2\mathrm{Li}_2\left(1-(t-m^2+i\eta)f^m\right)-2\mathrm{Li}_2\left(1-(s+i\eta)f^m\right)\Bigg],
\end{aligned} \tag{137}$$

where $f^m = \frac{s+t-m_1^2-m_3^2}{m^2(m_1^2-s)+st-m_1^2m_3^2}$.

The case $m_1^2 = 0$ gives rise to further divergences and has to be considered separately:

$$\begin{aligned}
I_4(s,t,m_1^2=0,m_3^2,m^2) &= \frac{i}{(4\pi)^2}\frac{\Gamma(1+\epsilon)(4\pi\mu^2)^\epsilon}{s(m^2-t)} \\
\times\Bigg[&-\frac{3}{2\epsilon^2}+\frac{1}{\epsilon}\left(2\ln(m^2-t-i\eta)-\frac{1}{2}\ln(m^2-i\eta)+\ln(-s-i\eta)-\ln(m^2-m_3^2-i\eta)\right) \\
&+\frac{2\pi^2}{3}+\frac{1}{4}\ln^2(m^2-i\eta)-\ln^2(m^2-t-i\eta)+\ln^2(m^2-m_3^2-i\eta)-\ln^2(-s-i\eta) \\
&+\ln(m^2-i\eta)\left(\ln(-s-i\eta)-\ln(m^2-m_3^2-i\eta)\right) \\
&-2\mathrm{Li}_2\left(1-\frac{m^2-m_3^2-i\eta}{-s-i\eta}\right)+2\mathrm{Li}_2\left(1-(m_3^2-m^2+i\eta)f^m\right) \\
&-2\mathrm{Li}_2\left(1-(t-m^2+i\eta)f^m\right)-2\mathrm{Li}_2\left(1-(s+i\eta)f^m\right)\Bigg],
\end{aligned} \tag{138}$$

where $f^m = \frac{s+t-m_3^2}{s(t-m^2)}$.

References

[1] M. Beneke, G. Buchalla, M. Neubert and C. T. Sachrajda, Phys. Rev. Lett. **83**, 1914 (1999).

[2] M. Beneke, G. Buchalla, M. Neubert and C. T. Sachrajda, Nucl. Phys. **B591**, 313 (2000).

[3] M. Beneke and S. Jäger, Nucl. Phys. **B751**, 160 (2006).

[4] N. Kivel, [hep-ph/0608291].

[5] C. W. Bauer, S. Fleming, D. Pirjol and I. W. Stewart, Phys. Rev. **D63**, 114020 (2001).

[6] C. W. Bauer, D. Pirjol and I. W. Stewart, Phys. Rev. **D65**, 054022 (2002).

[7] M. Beneke, A. P. Chapovsky, M. Diehl and T. Feldmann, Nucl. Phys. **B643**, 431 (2002).

[8] M. Beneke and S. Jäger, Nucl. Phys. **B768**, 51 (2007).

[9] G. Bell, [arXiv:0705.3133 [hep-ph]].

[10] G. Bell, [arXiv:0705.3127 [hep-ph]].

[11] G. Buchalla, A. J. Buras and M. E. Lautenbacher, Rev. Mod. Phys. **68**, 1125 (1996).

[12] M. Beneke, G. Buchalla, M. Neubert and C. T. Sachrajda, Nucl. Phys. **B606**, 245 (2001).

[13] M. Gronau, O. F. Hernandez, D. London and J. L. Rosner, Phys. Rev. **D50**, 4529 (1994).

[14] E. Remiddi, Nuovo Cim. **A110**, 1435 (1997).

[15] M. Caffo, H. Czyz, S. Laporta and E. Remiddi, Nuovo Cim. **A111**, 365 (1998).

[16] T. Gehrmann and E. Remiddi, Nucl. Phys. **B580**, 485 (2000).

[17] S. G. Gorishnii, Nucl. Phys. **B319**, 633 (1989).

[18] M. Beneke and V. A. Smirnov, Nucl. Phys. **B522**, 321 (1998).

[19] V. A. Smirnov, Commun. Math. Phys. **134**, 109 (1990).

[20] V. A. Smirnov, Springer Tracts Mod. Phys. **177**, 1 (2002).

[21] G. Duplančić and B. Nižić, Eur. Phys. J. **C20**, 357 (2001).

[22] K. G. Chetyrkin and F. V. Tkachov, Nucl. Phys. **B192**, 159 (1981).

[23] F. V. Tkachov, Phys. Lett. **B100**, 65 (1981).

[24] G. Passarino and M. J. G. Veltman, Nucl. Phys. **B160**, 151 (1979).

[25] V. Pilipp, [hep-ph/0703180].

[26] CKMfitter Group, J. Charles *et al.*, Eur. Phys. J. **C41**, 1 (2005), updates at `http://ckmfitter.in2p3.fr`.

[27] M. Jamin and B. O. Lange, Phys. Rev. **D65**, 056005 (2002).

[28] A. Khodjamirian, T. Mannel and N. Offen, [hep-ph/0611193].

[29] A. Abada *et al.*, Nucl. Phys. **B619**, 565 (2001).

[30] E. Dalgic *et al.*, Phys. Rev. **D73**, 074502 (2006).

[31] A. Khodjamirian, R. Rückl, S. Weinzierl, C. W. Winhart and O. I. Yakovlev, Phys. Rev. **D62**, 114002 (2000).

[32] M. Göckeler *et al.*, Nucl. Phys. Proc. Suppl. **161**, 69 (2006).

[33] V. M. Braun *et al.*, Phys. Rev. **D74**, 074501 (2006).

[34] Particle Data Group, W. M. Yao *et al.*, J. Phys. **G33**, 1 (2006), updates at `http://pdg.lbl.gov`.

[35] A. Khodjamirian, T. Mannel and N. Offen, Phys. Lett. **B620**, 52 (2005).

[36] V. M. Braun, D. Y. Ivanov and G. P. Korchemsky, Phys. Rev. **D69**, 034014 (2004).

[37] A. G. Grozin and M. Neubert, Phys. Rev. **D55**, 272 (1997).

[38] S. J. Lee and M. Neubert, Phys. Rev. **D72**, 094028 (2005).

[39] Heavy Flavor Averaging Group (HFAG), E. Barberio *et al.*, [hep-ex/0603003], updates at `http://www.slac.stanford.edu/xorg/hfag`.

[40] M. Beneke and M. Neubert, Nucl. Phys. **B675**, 333 (2003).